

Field theory for optimal signal propagation in ResNets

Kirsten Fischer,^{1,2,*} David Dahmen,¹ and Moritz Helias^{1,3}

¹*Institute for Advanced Simulation (IAS-6), Jülich Research Centre, Jülich, Germany*

²*RWTH Aachen University, Aachen, Germany*

³*Department of Physics, Faculty 1, RWTH Aachen University, Aachen, Germany*

(Dated: August 27, 2024)

Residual networks have significantly better trainability and thus performance than feed-forward networks at large depth. Introducing skip connections facilitates signal propagation to deeper layers. In addition, previous works found that adding a scaling parameter for the residual branch further improves generalization performance. While they empirically identified a particularly beneficial range of values for this scaling parameter, the associated performance improvement and its universality across network hyperparameters yet need to be understood. For feed-forward networks, finite-size theories have led to important insights with regard to signal propagation and hyperparameter tuning. We here derive a systematic finite-size field theory for residual networks to study signal propagation and its dependence on the scaling for the residual branch. We derive analytical expressions for the response function, a measure for the network's sensitivity to inputs, and show that for deep networks the empirically found values for the scaling parameter lie within the range of maximal sensitivity. Furthermore, we obtain an analytical expression for the optimal scaling parameter that depends only weakly on other network hyperparameters, such as the weight variance, thereby explaining its universality across hyperparameters. Overall, this work provides a theoretical framework to study ResNets at finite size.

I. INTRODUCTION

While feed-forward neural networks (FFNets) have proven successful at learning a multitude of tasks [1, 2], they become difficult to train at great depths [3]. As a result, very deep FFNets yield worse performance than their shallow counterparts. However, assuming adding layers with identity mappings to already successfully trained shallow networks, such a performance degradation should not be present. Therefore, [3, 4] introduced residual networks (ResNets) that contain skip connections directly connecting intermediate layers with identity mappings. Networks such as ResNet-50 [3] or ResNet-1001 [4] yield state-of-the-art performance on common benchmark data sets such as CIFAR-10 [5].

A scaling of the residual branch, i.e. of the non-identity mapping in each layer, was first introduced by Szegedy *et al.* [6] who found that for networks with large numbers of convolutional filters training becomes unstable and leads to inactive neurons. While this effect could not be mitigated by additional batch normalization [7], downscaling the residual branch by a value ρ between 0.1 and 0.3 proved to be a reliable solution. Finding the optimal residual scaling and a mechanistic explanation for its effectiveness remains an open question.

One line of research studies how such an optimal residual scaling depends on the network depth. From a kernel perspective, Huang *et al.* [8] argue that the Neural Tangent Kernel (NTK) in the double limit of infinite width and depth becomes degenerate for FFNets but not for ResNets, suggesting a polynomial scaling of the residual

branch with the inverse depth for better kernel stability at great depth. Bachlechner *et al.* [9] include the residual scaling as a trainable parameter and find that networks initialized at zero learn an inverse depth scaling.

According to Tirer *et al.* [10], smaller residual scalings lead to a smoother NTK and thereby to better interpolation properties between data points. Studying the spectral properties of the NTK, Barzilai *et al.* [11] find a bias of convolutional ResNets towards learning functions with low-frequency or localized over few pixels. Further, they show that the scaling proposed by Huang *et al.* [8] leads to a less expressive dot-product kernel for convolutional ResNets, therefore arguing for a depth-independent constant residual scaling. By performing a grid search, Zhang *et al.* [12] find a value near 0.1 to yield best generalization performance for deep ResNets.

[13–16] argue for a scaling by the square root of the inverse depth: Arpit *et al.* [13] use a mean field analysis to argue that this scaling avoids exploding or vanishing information in the forward and backward pass. While [14, 15] show that the resulting NTK is universal and can express any function, Zhang *et al.* [16] find that this scaling stabilizes forward and backward propagation. On the practical side, Bordelon *et al.* [17] show that scaling the residual branch by the square root of the inverse depth allows them to extend μP -scaling [18] to residual architectures.

We here tackle the problem of optimal scaling from a signal propagation perspective. We derive a field-theoretic description of residual networks to study their response function. This function describes the networks' sensitivity to varying inputs. As the network needs to be able to distinguish between different data samples, the overall range of output responses is a relevant indicator for both trainability and generalization. While

* ki.fischer@fz-juelich.de

a stronger signal generally ensures that two data samples can be better distinguished, this effect may be counteracted by saturation effects of the non-linearity in the residual branch of the network. The residual scaling parameter determines how strongly differences across data samples are amplified and propagated through the network.

Our main contributions are as follows

- we derive a novel field-theoretic description of the Bayesian network prior for residual networks that allows one to systematically account for finite-size properties of networks;
- we obtain the response function of residual networks as a finite-size effect that describes the networks' sensitivity to varying inputs;
- we show that the response function of the network output as a function of the residual scaling parameter has a distinct maximum and that the corresponding optimal residual scaling lies precisely within the value range empirically found by Szegedy *et al.* (2017);
- we derive the dependence of the optimal residual scaling on network hyperparameters and find a strong dependence on the network depth and weak dependence on all other hyperparameters, explaining the universality of a $1/\sqrt{\text{depth}}$ scaling for deep residual networks.

The field-theoretic framework for the Bayesian network prior can be generalized beyond ResNets and generally used to systematically take into account finite-size properties of neural networks. It thus holds potential beyond the content of this work.

The main part is structured into two parts: In Section II, we first derive a field-theoretic formulation of residual networks. In this field-theoretic framework, we recover the NNGP as a saddle point at infinite width and obtain the response function of residual networks as a finite-width correction to this saddle point. In Section III, we then study the behavior of the response function as a function of the residual scaling and find a unique maximum of the response close to the empirically found optimal values. Finally, we relate this scaling to optimal signal propagation that is bounded by saturation effects of the non-linearity and study its dependence on hyperparameters of the network.

II. FIELD THEORY OF RESIDUAL NETWORKS

We here study the following residual architecture

$$\begin{aligned} h^{(0)} &= W^{\text{in}}x + b^{\text{in}}, \\ h^{(l)} &= h^{(l-1)} + \rho [W^{(l)}\phi(h^{(l-1)}) + b^{(l)}] \quad l = 1, \dots, L, \\ y &= W^{\text{out}}\phi(h^{(L)}) + b^{\text{out}}, \end{aligned} \quad (1)$$

yielding a mapping from the input $x \in \mathbb{R}^{d_{\text{in}}}$ to the output $y \in \mathbb{R}^{d_{\text{out}}}$ as $x \mapsto f(x; \theta) = y$ with trainable network parameters $\theta = \{W^{\text{in}}, b^{\text{in}}, W^{(l)}, b^{(l)}, W^{\text{out}}, b^{\text{out}}\}$. Similar to state-of-the-art models such as ResNet-50 [3], the model contains a linear readin and a fully-connected readout layer. Thereby, the input $x \in \mathbb{R}^{d_{\text{in}}}$, the signal $h^{(l)} \in \mathbb{R}^N$, and the output $y \in \mathbb{R}^{d_{\text{out}}}$ can have different dimensions. We refer to the residual branch $\mathcal{F}(h^{(l-1)}) = \rho [W^{(l)}\phi(h^{(l-1)}) + b^{(l)}]$ together with the skip connection $h^{(l-1)}$ in Eq. (1) as a network layer with index l (see Fig. 1(a)). The total number of layers is given by L . We assume the non-linear activation function ϕ to be saturating and twice differentiable almost everywhere; two common choices satisfying both conditions are the logistic function and the error function. In the following, we use $\phi = \text{erf}$. The residual branch is multiplied by a scaling factor ρ , which is referred to as the residual scaling parameter in the following. We study networks at initialization, which is equivalent to determining the network prior in a setting of Bayesian inference. To this end, we assume that the network parameters are Gaussian distributed: For the input layer $W_{ij}^{\text{in}} \stackrel{\text{i.i.d.}}{\sim} \mathcal{N}(0, \sigma_{w,\text{in}}^2/d_{\text{in}})$, $b_i^{\text{in}} \stackrel{\text{i.i.d.}}{\sim} \mathcal{N}(0, \sigma_{b,\text{in}}^2)$, for residual layers $W_{ij}^{(l)} \stackrel{\text{i.i.d.}}{\sim} \mathcal{N}(0, \sigma_w^2/N)$, $b_i^{(l)} \stackrel{\text{i.i.d.}}{\sim} \mathcal{N}(0, \sigma_b^2)$, and for the readout layer $W_{ij}^{\text{out}} \stackrel{\text{i.i.d.}}{\sim} \mathcal{N}(0, \sigma_{w,\text{out}}^2/N)$, $b_i^{\text{out}} \stackrel{\text{i.i.d.}}{\sim} \mathcal{N}(0, \sigma_{b,\text{out}}^2)$.

A. Network prior in field-theoretic framework

We determine the network prior for the residual network model defined in Eq. (1). This derivation uses the field-theoretic approach employed in Segadlo *et al.* [19] to study deep feed-forward and recurrent networks and extends it to residual networks. Given a set of inputs $X = (x_\alpha)_{\alpha=1,\dots,P}$, the network prior $p(Y|X)$ describes the joint distribution of all outputs $Y = (y_\alpha)_{\alpha=1,\dots,P}$; each output y_α corresponds to one input x_α . Calculating the network prior jointly for all inputs x_α is analogous to the replica calculation in physics [20, 21]: for each input x_α one considers a copy of the network with the same network parameters θ shared across all of these replica. Here, we showcase the derivation of $p(x|y)$ for a single input x , dropping the sample indices for simplicity. The general case of P inputs follows the same arguments and is given in Appendix A.

The network prior is defined as the probability of an output y given an input x marginalized over the distribution of network parameters

$$p(y|x) = \int d\theta p(y|x, \theta) p(\theta). \quad (2)$$

Given fixed network parameters θ , the probability $p(y|x, \theta)$ is given by enforcing the network model with

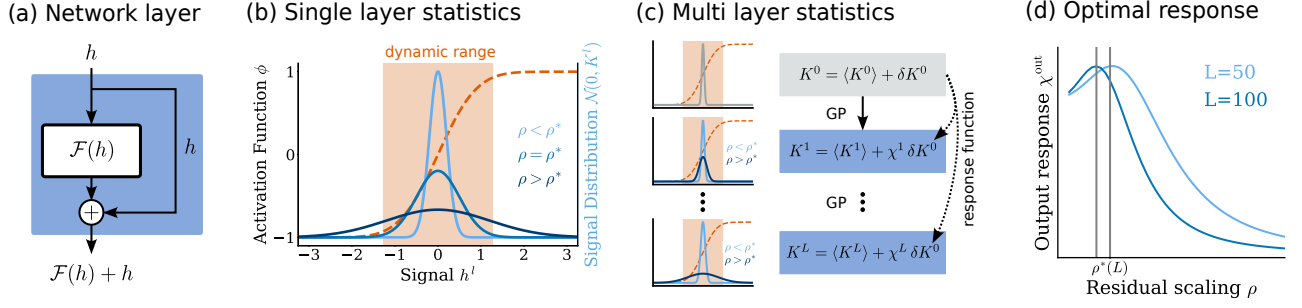


Figure 1. Signal distribution in residual network. (a) Network layer with residual branch and skip connection. The residual branch returns $h \mapsto \mathcal{F}(h)$, the layer passes on $\mathcal{F}(h) + h$ to the next layer. (b) Distribution of the signal $h^{(l)}$ after layer l (solid curves) relative to the dynamic range \mathcal{V} (shaded orange area) of the activation function $\phi = \text{erf}$ (dashed curve). The signal is Gaussian distributed $h^{(l)} \sim \mathcal{N}(0, K^{(l)})$ with variance given by $K^{(l)}$, which depends on the residual scaling parameter ρ . For values larger than the optimal scaling $\rho > \rho^*$, part of the signal is lost in the saturation of the activation function ϕ (dark blue). For values smaller than the optimal scaling $\rho < \rho^*$, the signal is restricted to a small fraction of the dynamic range (light blue) in which the activation function is typically linear. For optimal scaling $\rho = \rho^*$, the signal optimally utilizes the whole dynamic range \mathcal{V} of the activation function ϕ (blue). (c) The response function $\chi^{(l)}$ describes how the variance $K^{(l)}$, corresponding to the diagonal element of the GP kernel, changes to linear order in the perturbation of the input kernel $\delta K^{(0)}$ around its data mean $\langle K^{(0)} \rangle$. The kernel $K^{(l)}$ of the signal distribution can only increase across layers due to the skip connections; its rate of increase is governed by the residual scaling parameter ρ . If the signal goes into saturation ($\rho > \rho^*$) or remains close to zero ($\rho < \rho^*$), then the overall response of the network output to a change of the input kernel is limited. (d) The output response χ^{out} as a function of the residual scaling ρ exhibits a unique maximum that depends on the network depth L , yielding a scaling $\rho^*(L)$ that promotes optimal signal propagation in the network.

Dirac δ -distributions as

$$\begin{aligned}
 p(y|x, \theta) &= \int dh^{(0)} \dots \int dh^{(L)} \delta(h^{(0)} - W^{\text{in}}x - b^{\text{in}}) \\
 &\times \prod_{l=1}^L \delta(h^{(l)} - h^{(l-1)} - \rho W^{(l)} \phi(h^{(l-1)}) - \rho b^{(l)}) \\
 &\times \delta(y - W^{\text{out}} \phi(h^{(L)}) - b^{\text{out}}). \quad (3)
 \end{aligned}$$

Marginalization over network parameters

The marginalization over the network parameters is given by

$$\begin{aligned}
 p(y|x) &= \int dh^{(0)} \dots \int dh^{(L)} \langle \delta(h^{(0)} - W^{\text{in}}x - b^{\text{in}}) \rangle_{\{W^{\text{in}}, b^{\text{in}}\}} \\
 &\times \prod_{l=1}^L \langle \delta(h^{(l)} - h^{(l-1)} - \rho W^{(l)} \phi(h^{(l-1)}) - \rho b^{(l)}) \rangle_{\{W^{(l)}, b^{(l)}\}} \\
 &\times \langle \delta(y - W^{\text{out}} \phi(h^{(L)}) - b^{\text{out}}) \rangle_{\{W^{\text{out}}, b^{\text{out}}\}}, \quad (4)
 \end{aligned}$$

where $\langle \dots \rangle_{\{W, b\}}$ refers to the expectation value over the statistics of weights W and biases b and we use the shorthand $\phi^{(l)} = \phi(h^{(l)})$. We rewrite the Dirac δ -distributions using the Fourier representation

$$\delta(h) = \int d\tilde{h} \exp(\tilde{h}^\top h) \quad (5)$$

with scalar product $\tilde{h}^\top h = \sum_{i=1}^N \tilde{h}_i h_i$, integration measure $\int d\tilde{h} = \prod_k \int_{i \in \mathbb{R}} \frac{d\tilde{h}_k}{2\pi i}$ and \tilde{h} the conjugate variable to h . This yields

$$\begin{aligned}
 p(y|x) &= \int d\tilde{y} \int \mathcal{D}\tilde{h} \int \mathcal{D}h \langle \exp((\tilde{h}^{(0)})^\top (h^{(0)} - W^{\text{in}}x - b^{\text{in}})) \rangle_{\{W^{\text{in}}, b^{\text{in}}\}} \\
 &\times \prod_{l=1}^L \langle \exp((\tilde{h}^{(l)})^\top (h^{(l)} - h^{(l-1)} - \rho W^{(l)} \phi(h^{(l-1)}) - \rho b^{(l)})) \rangle_{\{W^{(l)}, b^{(l)}\}} \\
 &\times \langle \exp(\tilde{y}^\top (y - W^{\text{out}} \phi(h^{(L)}) - b^{\text{out}})) \rangle_{\{W^{\text{out}}, b^{\text{out}}\}}, \quad (6)
 \end{aligned}$$

where $\int \mathcal{D}h = \prod_{l=0}^L \int dh^{(l)}$ and $\int \mathcal{D}\tilde{h} = \prod_{l=0}^L \int d\tilde{h}^{(l)}$ for brevity. Since the network parameters θ are independently distributed, the integrals decouple and only integrals of the form $\int d\theta_k p(\theta_k) \exp(z\theta_k)$ appear, which can be solved exactly for $\theta_k \sim \mathcal{N}(0, \sigma^2)$ yielding $\exp(\frac{1}{2}\sigma^2 z^2)$. Rewriting the resulting terms as $\sum_{mn} [\tilde{y}_m \phi_n^{(L)}]^2 = \tilde{y}^\top \tilde{y} [\phi^{(L)}]^\top \phi^{(L)}$, allows us to compute the action \mathcal{S} of the network prior

$$p(y|x) = \int d\tilde{y} \int \mathcal{D}\tilde{h} \int \mathcal{D}h \exp(\mathcal{S}(y, \tilde{y}, h, \tilde{h}|x)),$$

where we distinguish between the contributions of the readin layer, the hidden layers of the network with residual connectivity, and the readout layer

$$\begin{aligned}
 \mathcal{S}(y, \tilde{y}, h, \tilde{h}|x) &= \mathcal{S}_{\text{in}}(h^{(0)}, \tilde{h}^{(0)}|x) + \mathcal{S}_{\text{net}}(h, \tilde{h}) \\
 &+ \mathcal{S}_{\text{out}}(y, \tilde{y}|h^{(L)}). \quad (7)
 \end{aligned}$$

These contributions are given by

$$\mathcal{S}_{\text{in}}(h^{(0)}, \tilde{h}^{(0)}|x) := [\tilde{h}^{(0)}]^\top h^{(0)} + \frac{1}{2} \frac{\sigma_{w,\text{in}}^2}{d_{\text{in}}} [\tilde{h}^{(0)}]^\top \tilde{h}^{(0)} x^\top x + \frac{1}{2} \sigma_{b,\text{in}}^2 [\tilde{h}^{(0)}]^\top \tilde{h}^{(0)}, \quad (8)$$

$$\mathcal{S}_{\text{net}}(h, \tilde{h}) := \sum_{l=1}^L [\tilde{h}^{(l)}]^\top [h^{(l)} - h^{(l-1)}] + \frac{1}{2} \rho^2 \frac{\sigma_w^2}{N} [\tilde{h}^{(l)}]^\top \tilde{h}^{(l)} [\phi^{(l-1)}]^\top \phi^{(l-1)} + \frac{1}{2} \rho^2 \sigma_b^2 [\tilde{h}^{(l)}]^\top \tilde{h}^{(l)}, \quad (9)$$

$$\mathcal{S}_{\text{out}}(y, \tilde{y}|h^{(L)}) := \tilde{y}^\top y + \frac{1}{2} \frac{\sigma_{w,\text{out}}^2}{N} \tilde{y}^\top \tilde{y} [\phi^{(L)}]^\top \phi^{(L)} + \frac{1}{2} \sigma_{b,\text{out}}^2 \tilde{y}^\top \tilde{y}. \quad (10)$$

In contrast to feed-forward networks, the conjugate variable $\tilde{h}^{(l)}$ of layer l does not only couple to the signal $h^{(l)}$ of layer l , but also to the signal $h^{(l-1)}$ of the previous layer $l-1$. This coupling across layers results from the skip connections in residual networks. The interdependence between layers induced by the coupling prohibits the marginalization over the intermediate signals $h^{(l)}$ in a direct manner as in feed-forward networks [19].

Auxiliary variables

Quadratic terms in h and \tilde{h} can be solved as Gaussian integrals. However, in Eq. (8)-(10) terms proportional to $\propto [\tilde{h}^{(l)}]^\top \tilde{h}^{(l)} [\phi^{(l-1)}]^\top \phi^{(l-1)}$ appear, which are at least quartic in h and \tilde{h} . To treat these terms, we introduce auxiliary variables

$$C^{(0)} := \frac{\sigma_{w,\text{in}}^2}{d_{\text{in}}} x^\top x + \sigma_{b,\text{in}}^2, \\ C^{(l)} := \rho^2 \frac{\sigma_w^2}{N} [\phi^{(l-1)}]^\top \phi^{(l-1)} + \rho^2 \sigma_b^2 \quad l = 1, \dots, L,$$

$$C^{(L+1)} := \frac{\sigma_{w,\text{out}}^2}{N} [\phi^{(L)}]^\top \phi^{(L)} + \sigma_{b,\text{out}}^2.$$

For wide networks $N \gg 1$, we expect the empirical average $\frac{1}{N} \sum_{i=1}^N [\phi_i^{(l-1)}]^2$ to concentrate around its mean value. Based on this intuition, we aim to rewrite the network prior $p(y|x)$ in terms of these scalar variables.

We enforce these definitions with Dirac δ -distributions as in Eq. (3). Then the scalar variables C and its conjugate variables \tilde{C} only couple to sums of \tilde{h} and $\phi(h)$ over all neuron indices, so that all components of h and \tilde{h} are identically distributed. Thus, we can rewrite the expression in scalar variables h and \tilde{h} , pulling out a factor N in all terms. For the input layer, we denote the ratio $d_{\text{in}}/N = \nu_0$ and set $\nu_l = 1$ for $l > 0$; different network widths N_l can be considered by setting $\nu_l = N_l/N$. Moving all integrals over scalar variables h and \tilde{h} to the exponent, we can write the network prior in terms of the auxiliary variables

$$p(y|x) = \int d\tilde{y} \left(\exp \left(\tilde{y}^\top y + \frac{1}{2} C^{(L+1)} \tilde{y}^\top \tilde{y} \right) \right)_{C, \tilde{C}}, \quad (11)$$

where $(C, \tilde{C}) \sim \exp(\mathcal{S}(C, \tilde{C}))$ with

$$\mathcal{S}(C, \tilde{C}) := -N \sum_{l=1}^{L+1} \nu_l C^{(l)} \tilde{C}^{(l)} + N \mathcal{W}(\tilde{C}|C), \\ \mathcal{W}(\tilde{C}|C) := \ln \prod_{l=1}^L \int dh^{(l)} \int d\tilde{h}^{(l)} \exp \left(\tilde{h}^{(l)} [h^{(l)} - h^{(l-1)}] + \frac{1}{2} C^{(l)} [\tilde{h}^{(l)}]^2 \right) \\ \times \exp \left(\tilde{C}^{(l)} \left[\rho^2 \sigma_w^2 \phi^{(l-1)} \phi^{(l-1)} + \rho^2 \sigma_b^2 \right] \right) \\ \times \exp \left(\tilde{C}^{(L+1)} \left[\sigma_{w,\text{out}}^2 \phi^{(L)} \phi^{(L)} + \sigma_{b,\text{out}}^2 \right] \right) \\ \times \int dh^{(0)} \int d\tilde{h}^{(0)} \exp \left(\tilde{h}^{(0)} h^{(0)} + \frac{1}{2} C^{(0)} [\tilde{h}^{(0)}]^2 + \tilde{C}^{(0)} \left[\frac{\sigma_{w,\text{in}}^2}{N} x^\top x + \nu_0 \sigma_{b,\text{in}}^2 \right] \right).$$

Saddle point approximation yields NNGP

The action \mathcal{S} scales with the network width N . In the limit of infinite width $N \rightarrow \infty$, we can thus perform a

saddle point approximation to evaluate integrals of the

form

$$\int \mathcal{D}C \int \mathcal{D}\tilde{C} f(C, \tilde{C}) \exp(\mathcal{S}(C, \tilde{C})) \stackrel{N \rightarrow \infty}{=} f(C_*, \tilde{C}_*),$$

where C_* and \tilde{C}_* are the saddle points of the action \mathcal{S} .

We compute the saddle points using the conditions

$$\frac{\partial \mathcal{S}}{\partial C} \stackrel{!}{=} 0, \quad \frac{\partial \mathcal{S}}{\partial \tilde{C}} \stackrel{!}{=} 0,$$

and get

$$C_*^{(l)} = \begin{cases} \frac{\sigma_{w,\text{in}}^2}{d_{\text{in}}} x^\top x + \sigma_{b,\text{in}}^2 & l = 0, \\ \rho^2 \sigma_w^2 \langle \phi^{(l-1)} \phi^{(l-1)} \rangle_p + \rho^2 \sigma_b^2 & 1 \leq l \leq L, \\ \sigma_{w,\text{out}}^2 \langle \phi^{(L)} \phi^{(L)} \rangle_p + \sigma_{b,\text{out}}^2 & l = L + 1, \end{cases}$$

$$\tilde{C}_*^{(l)} = 0 \quad l = 0, \dots, L + 1,$$

where

$$\begin{aligned} \langle \dots \rangle_p &= \int dh^{(0)} \int d\tilde{h}^{(0)} \exp\left(\tilde{h}^{(0)} h^{(0)} + \frac{1}{2} C_*^{(0)} [\tilde{h}^{(0)}]^2\right) \\ &\times \prod_{l=1}^L \int dh^{(l)} \int d\tilde{h}^{(l)} \dots \exp\left(\tilde{h}^{(l)} [h^{(l)} - h^{(l-1)}] + \frac{1}{2} C_*^{(l)} [\tilde{h}^{(l)}]^2\right). \end{aligned}$$

For brevity, we also include the input kernel $C_*^0 = C^0$ here, which is fixed by the data. The appearing expectation values are computed self-consistently with respect to C_*^l .

By defining the residual $f^{(l)} = h^{(l)} - h^{(l-1)}$ for $1 \leq l \leq L$, we rewrite the appearing average as

$$\begin{aligned} \langle \dots \rangle_p &= \int dh^{(0)} \int d\tilde{h}^{(0)} \exp\left(\tilde{h}^{(0)} h^{(0)} + \frac{1}{2} C_*^{(0)} [\tilde{h}^{(0)}]^2\right) \\ &\times \prod_{l=1}^L \int df^{(l)} \int d\tilde{h}^{(l)} \dots \exp\left(\tilde{h}^{(l)} f^{(l)} + \frac{1}{2} C_*^{(l)} [\tilde{h}^{(l)}]^2\right) \quad (12) \\ &= \int dh^{(0)} \mathcal{N}(h^{(0)} | 0, C_*^{(0)}) \prod_{l=1}^L \int df^{(l)} \dots \mathcal{N}(f^{(l)} | 0, C_*^{(l)}), \quad (13) \end{aligned}$$

where $\mathcal{N}(f^{(l)} | 0, C_*^{(l)})$ denotes a Gaussian with zero mean and covariance $C_*^{(l)}$. From the latter expression follows that the residuals $f^{(l)}$ for $1 \leq l \leq L$ and $h^{(0)}$ are Gaussian distributed with covariance $C_*^{(l)}$ in the saddle point approximation. Since the residuals $f^{(l)}$ are independent Gaussians, the signal $h^{(l)}$ is also Gaussian distributed with covariance $K^{(l)} = \sum_{k=0}^l C_*^{(k)}$.

Thus, we obtain

$$C_*^{(l)} = \rho^2 \sigma_w^2 \langle \phi^{(l-1)} \phi^{(l-1)} \rangle_{\mathcal{N}(0, K^{(l-1)})} + \rho^2 \sigma_b^2, \quad (14)$$

$$K^{(l)} = \begin{cases} \frac{\sigma_{w,\text{in}}^2}{d_{\text{in}}} x^\top x + \sigma_{b,\text{in}}^2 & l = 0, \\ \sum_{k=0}^l C_*^{(k)} & 1 \leq l \leq L, \\ \sigma_{w,\text{out}}^2 \langle \phi^{(L)} \phi^{(L)} \rangle_{\mathcal{N}(0, K^{(L)})} + \sigma_{b,\text{out}}^2 & l = L + 1. \end{cases} \quad (15)$$

We recover the known NNGP result for the kernels as $K^{(l)} = K^{(l-1)} + C_*^{(l)}$ [8, 10, 11].

B. Next-to-leading-order correction yields response function

The strength of the here employed field-theoretic formalism is that finite-size corrections to the NNGP result (15) can be systematically calculated. For finite-size networks, the residual kernels $C^{(l)}$ fluctuate around the above saddle point value. To lowest-order, we describe these fluctuations as Gaussian. We obtain these by computing the Hessian of the action \mathcal{S} at the saddle point. Hence, all following expectation values are with respect to the measure $\langle \dots \rangle_p$ defined in Eq. (12). The diagonal terms are given by

$$\begin{aligned} \frac{\partial^2}{\partial C^{(l)} \partial C^{(k)}} \mathcal{S} &= 0, \\ \frac{\partial^2}{\partial \tilde{C}^{(l)} \partial \tilde{C}^{(k)}} \mathcal{S} &= N \sigma_w^4 1_{l>0} 1_{k>0} \langle \phi^{(l-1)} \phi^{(l-1)}, \phi^{(k-1)} \phi^{(k-1)} \rangle_p^c \\ &\times \begin{cases} \rho^4 & k, l \neq L + 1, \\ \rho^2 & k \neq l = L + 1 \vee l \neq k = L + 1, \\ 1 & \text{else,} \end{cases} \end{aligned}$$

where $1_{l>0}$ denotes the indicator function. We write $\langle \dots \rangle^c$ for connected correlations defined as

$$\begin{aligned} \langle \phi^{(l-1)} \phi^{(l-1)}, \phi^{(k-1)} \phi^{(k-1)} \rangle_p^c &= \langle \phi^{(l-1)} \phi^{(l-1)} \phi^{(k-1)} \phi^{(k-1)} \rangle_p - \langle \phi^{(l-1)} \phi^{(l-1)} \rangle_p \langle \phi^{(k-1)} \phi^{(k-1)} \rangle_p. \end{aligned}$$

For the off-diagonal terms, we have

$$\begin{aligned} \frac{\partial^2}{\partial C^{(l)} \partial \tilde{C}^{(k)}} \mathcal{S} &= -N \nu_l \delta_{kl} \\ &+ N 1_{k>0} \sigma_w^2 \langle [\phi^{(l-1)}, \phi^{(k-1)}]^2 + \phi^{(l-1), (k-1)} \phi^{(k-1)} \rangle_{\mathcal{N}(0, K^{(k-1)})} 1_{k>l} \\ &\times \begin{cases} \rho^2 & k \leq L \\ 1 & k = L + 1 \end{cases}, \end{aligned} \quad (16)$$

where we used Price's theorem [22] to compute the derivative of the expectation value by the covariance. The condition $k > l$ enforced by the indicator function $1_{k>l}$ results from the term $\frac{\partial}{\partial C^{(l)}} K^{(k-1)}$, because the network kernel $K^{(k-1)}$ only depends on the residual kernels $C^{(l)}$ with $l < k$.

Altogether, we get

$$\mathcal{S}^{(2)} = \begin{pmatrix} \frac{\partial^2}{\partial C^2} \mathcal{S} & \frac{\partial^2}{\partial C \partial \tilde{C}} \mathcal{S} \\ \frac{\partial^2}{\partial \tilde{C} \partial C} \mathcal{S} & \frac{\partial^2}{\partial \tilde{C}^2} \mathcal{S} \end{pmatrix} = \begin{pmatrix} \mathcal{S}_{11} & \mathcal{S}_{12} \\ \mathcal{S}_{21} & \mathcal{S}_{22} \end{pmatrix}.$$

We obtain the Gaussian fluctuations of the variables $C^{(l)}$ and $\tilde{C}^{(l)}$ by taking the negative inverse of the Hessian, also called the propagator in field theory

$$\Delta = -(\mathcal{S}^{(2)})^{-1} = \begin{pmatrix} \Delta_{11} & \Delta_{12} \\ \Delta_{21} & \Delta_{22} \end{pmatrix}.$$

By using the block structure and the fact that $\mathcal{S}_{11} = 0$, we have

$$\Delta_{11} = \Delta_{12} \mathcal{S}_{22} \Delta_{21}, \quad (17)$$

$$\Delta_{12} = -\mathcal{S}_{21}^{-1}, \quad (18)$$

$$\Delta_{22} = 0. \quad (19)$$

Since the off-diagonal block matrix \mathcal{S}_{21} is a lower triangular matrix, its inverse can be computed using forward propagation

$$\begin{aligned} \Delta_{12}^{lm} &= N^{-1} \nu_l^{-1} \delta_{lm} \\ &+ 1_{l>0} \sigma_w^2 \langle [\phi'^{(k-1)}]^2 + \phi''^{(k-1)} \phi^{(k-1)} \rangle_{\mathcal{N}(0, K^{(l-1)})} \sum_{k=0}^{l-1} \Delta_{12}^{km} \\ &\times \begin{cases} \rho^2 & k \leq L \\ 1 & k = L+1 \end{cases}, \end{aligned}$$

yielding $\Delta_{12}^{lm} = \text{Cov}(C^{(l)}, \tilde{C}^{(m)})$ as the forward response function in layer l to a perturbation of the residual in layer m . Here, we derive it as a $\mathcal{O}(N^{-1})$ correction to the NNGP result. Due to the residual architecture, any response can only propagate forward in the network, which is reflected in the term $1_{k>l}$ in Eq. (16). The kernel $K^{(l)}$ in layer l depends explicitly not only on the kernel of the previous layer as for FFNets but on all preceding layers. This property directly results from the skip connections in residual networks. Thereby, the response function in layer l contains information from all preceding layers, such that information can propagate to deeper network layers.

We are ultimately interested in the response with respect to the network input. For the response of the residual kernels $C^{(l)}$ in all intermediate layers $0 < l < L+1$, we have

$$\eta^{(l)} = \rho^2 \sigma_w^2 \langle [\phi'^{(k-1)}]^2 + \phi''^{(k-1)} \phi^{(k-1)} \rangle_{\mathcal{N}(0, K^{(l-1)})} \sum_{k=0}^{l-1} \eta^{(k)}. \quad (20)$$

Due to their additive nature, the response of the kernels $K^{(l)}$ is given by $\chi^{(l)} = \sum_{k=0}^l \chi^{(k)}$. Finally, the output response is given by

$$\chi^{\text{out}} = \sigma_{w, \text{out}}^2 \langle [\phi^{(L)}]' [\phi^{(L)}]' + [\phi^{(L)}]'' [\phi^{(L)}] \rangle_{\mathcal{N}(0, K^{(L)})} \sum_{k=0}^L \eta^{(k)}. \quad (21)$$

In addition, one can also compute the fluctuation corrections from the Hessian via Eq. (17). For details, see Appendix B.

In Fig. 2 we compare the behavior of the residual kernels $C_*^{(l)}$ and the response function $\eta^{(l)}$ between FFNets and ResNets. While the residual kernels $C_*^{(l)}$ in FFNets decay to zero as a function of depth, they approach a value larger than zero in ResNets due to the accumulation of variance across layers. Similarly, while the response function in FFNets decays exponentially to zero, it decays much slower in ResNets and approaches zero only asymptotically (see Appendix D A). The latter observation matches previous results by [23] based on the

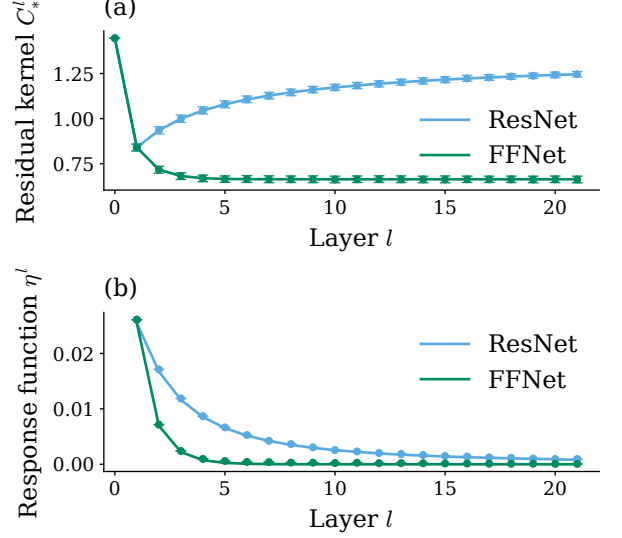


Figure 2. Residual kernels $C_*^{(l)}$ (a) and the respective response function $\eta^{(l)}$ (b) in ResNets (blue) compared to FFNets (green). In (a) error bars indicate standard error of the mean obtained from simulation over 10^3 network initializations, solid curves show theory values Eq. (14). In (b) dots represent simulations over 10^2 input samples and 10^3 network initializations, solid curves show theory values Eq. (20). Errors are of order 10^{-5} and therefore not shown. ResNets exhibit a slower decay over layers l compared to FFNets. Other parameters: $\sigma_{w, \text{in}}^2 = \sigma_w^2 = \sigma_{w, \text{out}}^2 = 1.2$, $\sigma_{b, \text{in}}^2 = \sigma_b^2 = \sigma_{b, \text{out}}^2 = 1.2$, $d_{\text{in}} = d_{\text{out}} = 100$, $N = 500$, $\rho = 1$.

convergence rate of the kernels; however, we here derive the response function that explicitly measures the dependence on the input kernel.

C. Relation to linear response theory

In the previous section, we derive the response function of the network as the first-order approximation in $\mathcal{O}(N^{-1})$ from a systematic field-theoretic calculation. The field-theoretic approach has the advantage of providing a framework in which we can systematically compute such correction terms to different orders; to provide more intuition on the response function we here discuss its relation to linear response theory.

Consider a change of the input kernel given by $K^{(0)} = \langle K^{(0)} \rangle + \delta K^{(0)}$. For small perturbations $\delta K^{(0)}$, we can ask how kernels in subsequent layers are affected by this perturbation. To linear order in $\delta K^{(0)}$, we expand the residual kernel as

$$C_*^{(l)} = C_*^{(l)}|_{\langle K^{(0)} \rangle} + \frac{\partial C_*^{(l)}}{\partial K^{(0)}}|_{\langle K^{(0)} \rangle} \delta K^{(0)} + \mathcal{O}(\delta^2).$$

The first-order Taylor term accounts for the effect of the

perturbation and corresponds to the response function

$$\begin{aligned}\eta^{(l)} &= \frac{\partial C^{(l)}}{\partial K^{(0)}}|_{\langle K^{(0)} \rangle} \\ &= \rho^2 \sigma_w^2 \frac{\partial}{\partial K^{(l-1)}} \langle \phi^{(l-1)} \phi^{(l-1)} \rangle_{\mathcal{N}(0, K^{(l-1)})} \frac{\partial K^{(l-1)}}{\partial K^{(0)}}|_{\langle K^{(0)} \rangle} \\ &= \rho^2 \sigma_w^2 \left([\phi'^{(l-1)}]^2 + \phi''^{(l-1)} \phi^{(l-1)} \right)_{\mathcal{N}(0, K^{(l-1)})} \sum_{k=0}^{l-1} \eta^{(k)},\end{aligned}$$

where we used Price's theorem [22] from the second to the third line and $\frac{\partial K^{(l-1)}}{\partial K^{(0)}}|_{\langle K^{(0)} \rangle} = \sum_{k=0}^{l-1} \frac{\partial C^{(k)}}{\partial K^{(0)}}|_{\langle K^{(0)} \rangle} = \sum_{k=0}^{l-1} \eta^{(k)}$ in the last line. The expectation value of the derivatives $\langle [\phi'^{(l-1)}]^2 + \phi''^{(l-1)} \phi^{(l-1)} \rangle_{\mathcal{N}(0, K^{(l-1)})}$ measures how the perturbation of the kernel $K^{(l-1)}$ affects the residual kernel $C_*^{(l)}$ in the subsequent layer l . It gets multiplied by the accumulated perturbations of all previous layers, as one expects intuitively due to the skip connections in residual networks. The expression for the linear response of the kernels $K^{(l)}$ follows directly from its definition

$$\chi^{(l)} = \frac{\partial K^{(l)}}{\partial K^{(0)}}|_{\langle K^{(0)} \rangle} = \frac{\partial}{\partial K^{(0)}} \sum_{k=0}^l C_*^{(k)}|_{\langle K^{(0)} \rangle} = \sum_{k=0}^l \eta^{(k)}.$$

While expressions for the response function can be computed using linear response theory, the field-theoretic formalism in Section II B formally shows that the response function is the leading order $\mathcal{O}(N^{-1})$ finite-size correction to the NNGP result.

III. SIGNAL PROPAGATION AND OPTIMAL SCALING IN RESIDUAL NETWORKS

Next we apply the field-theoretic framework derived above to study signal propagation in ResNets. The sensitivity of signal propagation to different inputs can be measured by the response function [24]. Good signal propagation is linked to improved trainability and thus higher generalization performance of trained networks [23, 24]. We first focus on the behavior of the diagonal elements of the network kernels to obtain an intuition for the signal propagation in residual networks and then discuss how their behavior extends to off-diagonal elements of the network kernels.

A. Optimal scaling of the residual branch

We start by studying the effect of the residual scaling parameter ρ on the kernels $K^{(l)}$ and response function $\chi^{(l)}$ of layer l as these quantities describe the distribution of the signal $h^{(l)}$. Since ρ^2 scales the residual kernels $C_*^{(l)}$ in Eq. (14), which are being summed to obtain $K^{(l)}$, the residual scaling governs the rate of increase of $K^{(l)}$ across layers (see Fig. 3(a)). The response function $\chi^{(l)}$ exhibits the same scaling and thus behavior (see Fig. 3(b)).

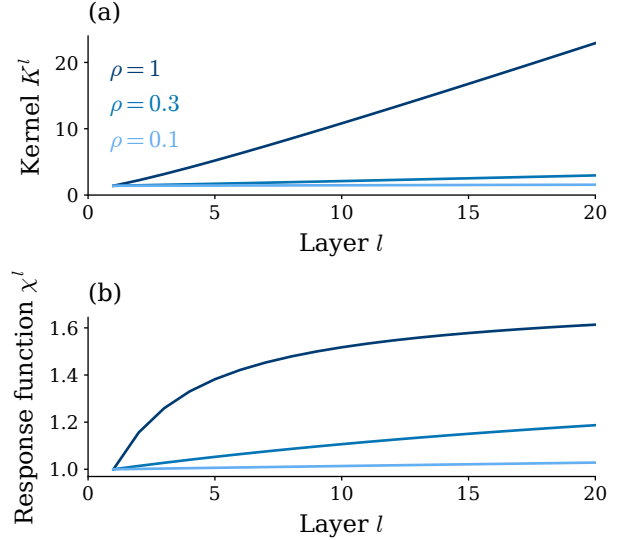


Figure 3. Dependence of (a) kernels $K^{(l)}$ and (b) the respective response function $\chi^{(l)}$ on residual scaling parameter ρ . The residual scaling takes values $\rho \in [1.0, 0.3, 0.1]$ (from dark to light). The residual scaling parameter ρ governs the rate of increase in both quantities. Other parameters: $\sigma_{w,\text{in}}^2 = \sigma_w^2 = \sigma_{w,\text{out}}^2 = 1.2$, $\sigma_{b,\text{in}}^2 = \sigma_b^2 = \sigma_{b,\text{out}}^2 = 0.2$, $d_{\text{in}} = d_{\text{out}} = 100$, $N = 500$.

The dependence of the residual kernels $C_*^{(l)}$ on the residual scaling ρ transfers to the response function; in particular the output response shown in Fig. 4(a)-(b) exhibits a unique maximum ρ^* . The shape of the response function and thus the optimal value ρ^* depend on the network depth L , shifting to smaller values ρ^* with larger depth. However, we observe an antagonistic effect: the depth dependence becomes weaker for deeper networks. The optimal value ρ^* lies between $[0.1, 0.3]$, as found empirically in previous works [6, 12].

Due to the recursive nature of the non-linear Eqs. (20)-(21) for the response function, we cannot determine the optimal value ρ^* analytically. However, for the variance $K^{(l)}$ we can make an intuitive argument regarding the signal propagation in the network: For deeper networks the kernels $K^{(l)}$ in Eq. (15) grow continuously, so that the signal $h^{(l)}$ leaves the dynamic range \mathcal{V} of the activation function ϕ (see Fig. 1(b)). In consequence, part of the signal $h^{(L)}$ is lost in the readout layer, reducing the output response χ^{out} to changing inputs. The magnitude of the network kernels $K^{(l)}$ depends on ρ^2 , so that a smaller residual scaling leads to a less rapid growth of the kernels $K^{(l)}$ and the signal $h^{(L)}$ stays in the dynamic range \mathcal{V} . For very small scalings ρ , the residual branch is suppressed and the network reduces to a single layer perceptron (see Fig. 1(c)).

Based on this intuition, we obtain an approximate expression for the optimal scaling ρ^* : We assume that the signal $h^{(l)}$ stays in the dynamic range \mathcal{V} of the activa-

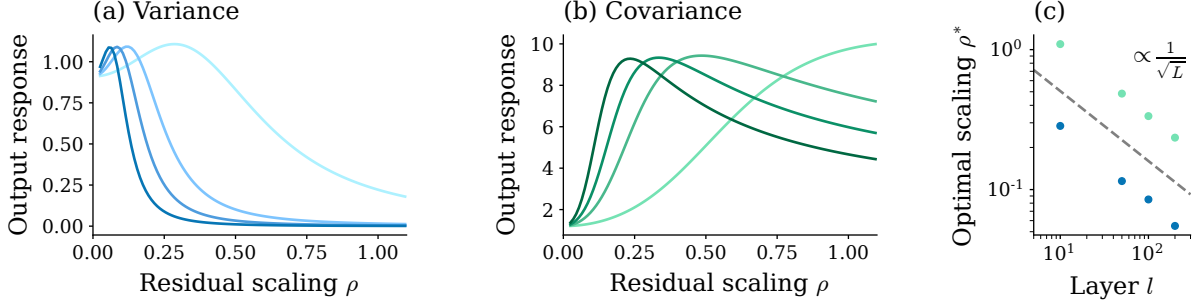


Figure 4. Optimal scaling of the residual branch. Output response χ^{out} for (a) diagonal and (b) off-diagonal elements of the network kernel $K_{\alpha\beta}^{(l)}$. Different curves correspond to different network depths $L \in [10, 50, 100, 200]$ (light to dark). All curves exhibit a unique maximum; the residual scaling values ρ^* with largest response concentrate with increasing depth. (c) Optimal residual scaling $\rho^* = \text{argmax}(\chi^{\text{out}})$ for diagonal (blue) and off-diagonal (green) elements of the network kernel $K_{\alpha\beta}^{(l)}$. In both cases, these scale with $1/\sqrt{L}$ (gray). Other parameters: input kernel $K^{(0)} = \begin{pmatrix} 0.05 & 0.03 \\ 0.03 & 0.05 \end{pmatrix}$, $\sigma_w^2 = 1.25$, $\sigma_b^2 = 0.05$, $d_{\text{in}} = d_{\text{out}} = 100$, $N = 500$.

tion function so that $\phi(h^{(l)}) \approx \phi'(0)h^{(l)}$, where $\phi'(0)$ accounts for the slope of the activation function at its origin. The residual kernel then simplifies to

$$C_*^{(l)} = \rho^2 \sigma_w^2 \phi'(0)^2 \sum_{k=0}^{l-1} C_*^{(k)} + \rho^2 \sigma_b^2,$$

and hence we get $C_*^{(l)} = C_*^{(l-1)} + \rho^2 \sigma_w^2 \phi'(0)^2 C_*^{(l-1)}$. Solving this recursion, we get

$$C_*^{(l)} = (1 + \rho^2 \sigma_w^2 \phi'(0)^2)^{l-1} (\rho^2 \sigma_w^2 \phi'(0)^2 K^{(0)} + \rho^2 \sigma_b^2).$$

Using the sum of the first $L+1$ terms of the geometric series and $C^{(0)} = K^{(0)}$ per definition, we obtain

$$\begin{aligned} K^L &= \sum_{k=0}^L C^{(k)} \\ &= (1 + \rho^2 \sigma_w^2 \phi'(0)^2)^L K^{(0)} \\ &\quad + \frac{\sigma_b^2}{\phi'(0)^2 \sigma_w^2} ((1 + \rho^2 \sigma_w^2 \phi'(0)^2)^L - 1). \end{aligned} \quad (22)$$

Assuming the σ -range of the distribution to stay within the dynamic range \mathcal{V} for a point-symmetric activation function ϕ , we set $\mathcal{V}/2 \stackrel{!}{=} \sqrt{K^{(L)}}$ and obtain for the optimal scaling parameter

$$\rho^* \approx \frac{1}{\sigma_w \phi'(0)} \sqrt{\left(\frac{\sigma_w^2 \phi'(0)^2 (\mathcal{V}/2)^2 + \sigma_b^2}{\sigma_w^2 \phi'(0)^2 K^{(0)} + \sigma_b^2} \right)^{\frac{1}{L}} - 1}. \quad (24)$$

The assumption $\mathcal{V}/2 \stackrel{!}{=} \sqrt{K^{(L)}}$ is only an estimate; multiple σ -ranges could be required for optimal signal propagation. Alternatively, we derive this condition from a maximum-entropy argument for the signal distribution (see Appendix C). A similar-maximum entropy argument has been used by Bukva *et al.* [25] to study trainability of feed-forward networks. Note that due to the assumptions

made in deriving this expression, it cannot fully capture the behavior of the signal when it reaches the non-linear part of the activation-function. However, this is solely a limitation of this particular ansatz to obtain an analytically tractable expression for ρ^* ; the response function itself captures all non-linear effects in the network.

B. Depth scaling dominates optimal scaling

At large depth L , the expression for optimal scaling in Eq. (24) is dominated by the appearing L -th root and can be written as

$$\rho^* \approx \sqrt{\frac{1}{L}} \sqrt{\frac{1}{\sigma_w^2 \phi'(0)^2} \log \left(\frac{\sigma_w^2 \phi'(0)^2 (\mathcal{V}/2)^2 + \sigma_b^2}{\sigma_w^2 \phi'(0)^2 K^{(0)} + \sigma_b^2} \right)}, \quad (25)$$

neglecting terms of order $\mathcal{O}(L^{-1})$. Thus, we obtain the proportionality of the optimal scaling value with $\propto 1/\sqrt{L}$ in Fig. 4(c); this scaling has been reported based on different approaches in earlier works [14–16]. In contrast to those works, we here also obtain the dependence on other hyperparameters of the network. While the scaling with $1/\sqrt{L}$ dominates, there's only a weak dependence on other hyperparameters due to the appearing logarithm as shown in Fig. 5. This weak dependence on network hyperparameters but strong dependence on network depth offers an explanation for the widespread success of the $1/\sqrt{L}$ scaling across different architectures [17].

C. Behavior across full data set

While the above considerations apply to the diagonal elements of the network kernels, i.e. for the statistics of a single sample, we require efficient signal propagation for all samples of a data set of size P . The joint statistics of multiple data samples cannot be analyzed with

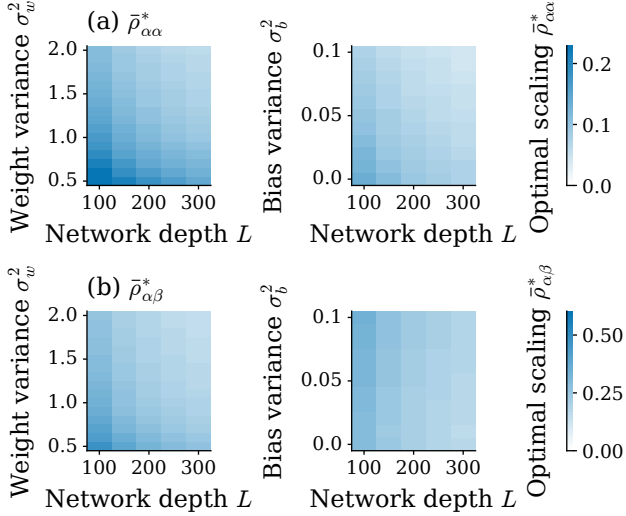


Figure 5. Optimal scalings depend strongly on network depth but weakly on other hyperparameters. We illustrate the weak dependence on the weight variance σ_w^2 and bias variance σ_b^2 relative to the network depth L for CIFAR-10 for both (a) variances and (b) covariances; samples are either dogs or airplanes. We measure the scaling with maximal output response averaged over all diagonal or all off-diagonal elements of the covariance, $\bar{\rho}_{\alpha\alpha}^* = \frac{1}{N} \sum_{\alpha} \text{argmax}(\chi_{\alpha\alpha}^{\text{out}})$ or $\bar{\rho}_{\alpha\beta}^* = \frac{1}{N(N-1)} \sum_{\alpha \neq \beta} \text{argmax}(\chi_{\alpha\beta}^{\text{out}})$. Other parameters: data set size $P = 20$, input scale $K^{(0)} = 0.05$, $\sigma_w^2 = 1.25$, $\sigma_b^2 = 0.05$, $d_{\text{in}} = d_{\text{out}} = 100$, $N = 500$.

the simplified intuition of saturation arguments and variances. The non-approximated field-theoretic result, however, still yields the behavior of the full covariances. The off-diagonal elements do not get a contribution from the term involving the second derivative in Eq. (24), which is negative for $\phi = \text{erf}$ and other saturating activation functions. In consequence, the response function for off-diagonal elements is larger and admits a larger residual scaling ρ .

To investigate the dependence of the optimal scaling with maximal output response $\rho^*(K_{\alpha\beta}) = \text{argmax}(\chi_{\alpha\beta}^{\text{out}})$ on differences in data samples, we generate samples of unit length and encode sample differences by angles that have an equal spacing in the range of $[0, 2\pi]$ by steps of $2\pi/P$. In Fig. 6(a), we observe a noticeable angular dependence of the optimal scaling. For common data sets such as MNIST and CIFAR-10, we find that optimal scalings $\rho^*(K_{\alpha\beta})$ for off-diagonal elements of the kernels behave rather homogeneously, even though samples stem from two different classes. Thus, the average scalings $\bar{\rho}^* = \frac{1}{N(N-1)} \sum_{\alpha \neq \beta} \text{argmax}(\chi_{\alpha\beta}^{\text{out}})$ for off-diagonal elements of each data set provide a good indicator for suitable values.

Further, we find the same $1/\sqrt{L}$ scaling of variances for the covariances in Fig. 4(c). Apart from this strong dependence on network depth, there is again only a weak dependence of the optimal scaling on other hyperparam-

eters (see Fig. 5(b)).

In summary, the response function, which naturally arises in a field-theoretic formulation of residual networks, predicts the dependence of optimal scaling ρ^* on all network hyperparameters and data statistics and thus provides a theoretical explanation for the empirically well-tested the $1/\sqrt{L}$ scaling.

IV. DISCUSSION

Understanding signal propagation in neural networks is essential for a theory of trainability and generalization. Regarding these points, residual networks have shown to be superior to feed-forward network [3, 4]; scaling the residual branches in ResNets further amplifies this effect [6]. We here derive a field-theoretic formulation of residual networks that allows us to determine finite-size corrections in a systematic way. The response function of residual networks, a measure for the network’s sensitivity to variability in the input and thus network trainability, naturally appears as the leading-order correction to the NNGP. We show that, in contrast to feed-forward networks, the response function decays to zero only asymptotically, consequently allowing information to propagate to very deep layers, in line with Yang and Schoenholz (2017). Further, we show that signal propagation in ResNets is optimal when the signal distribution utilizes the whole dynamic range of the activation function. Beyond this range, information is lost due to saturation effects. Finally, we are able to explain the universality of empirically found optimal values due to a weak dependence on all network hyperparameters but the network depth. Thereby, this work sheds light on the interplay between signal propagation, saturation effects and signal scales in residual networks.

Limitations Since we study the network prior of residual networks, the obtained results apply to networks at initialization. Despite this limitation, [23, 24] have shown that network trainability at initialization is a good indicator for generalization performance. Further, one needs the network prior in order to obtain the network posterior as well as posterior quantities such as the generalization performance.

The presented field-theoretic formalism allows the systematic computation of finite-size corrections from an expansion of the exact action. We here truncated this expansion at first order, which yields the response function. In general, higher orders may appear and are computationally more costly to obtain. By definition, these, however, do not alter the response function, which was studied in this work.

Related works Understanding the effect of skip connections in residual networks has been studied using different quantities: Building on the empirical observation that connections skipping a certain number of fully-connected layers lead to smaller training errors, Li *et al.* [26] show that the condition number of the Hessian of

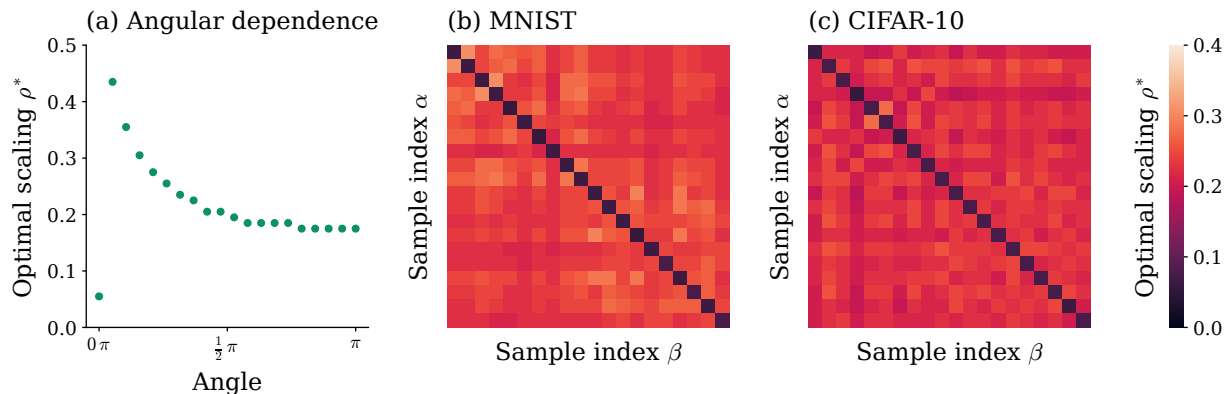


Figure 6. Dependence of optimal scaling ρ^* on sample variability. (a) Dependence of optimal scaling on the angle between normalized synthetic data samples. On common, real-world data sets such as (b) MNIST and (c) CIFAR-10, optimal scalings ρ^* for off-diagonal elements of the kernels (samples sorted by classes only) yield similar values across data samples. For MNIST we use samples from digit 0 and digit 3, and for CIFAR-10 samples are either dogs or airplanes. Other parameters: data set size $P = 20$, input scale $K^{(0)} = 0.05$, $\sigma_w^2 = 1.25$, $\sigma_b^2 = 0.05$, $d_{\text{in}} = d_{\text{out}} = 100$, $N = 500$.

the loss function does not grow with network depth but is depth-invariant. Further, ResNets achieve improved data separability compared to FFNets as they preserve angles between samples and thus exhibit less degradation of the ratio between within-class distance and between-class distance [27].

While we here explicitly focus on finite-size networks and the implications of the finite size, other works examine the scaling behavior in the infinite-size limit. Yang and Schoenholz [23] explicitly study signal propagation in residual networks in the infinite-width limit by determining the decay rate of sample correlations to their fixed point values. They find a sub-exponential or even polynomial decay, indicating that, in contrast to feed-forward networks [24, 28, 29], residual networks are always close to the edge of chaos, leading to better trainability also at great depth. We recover their result and go beyond it by investigating the effect of scaling the residual branch on signal propagation. The closeness to the edge of chaos they describe can be linked to the long depth scale and increased amplitude of the response function we demonstrate here.

Neural ODEs [30] consider the limit of infinite depth for residual networks, yielding a set of differential equations describing the network dynamics. Cohen *et al.* [31] find three different scaling regimes of neural ODEs depending on the choice of architecture and activation function. Barboni *et al.* provide global convergence guarantees for gradient descent and optimal transport training [32, 33]. Chen *et al.* [34] derive generalization bounds beyond the NTK regime. Li and Nica [35] find a connection between the infinite-depth and -width limits for residual networks with a scaling by square root of the inverse depth on the residual branches and feed-forward networks with activation functions scaled by the same factor, building on the $1/\sqrt{\text{depth}}$ scaling for which we here derive the theoretical basis. Marion *et al.* [36] find a

strong relationship between residual scaling and the regularity of the weights for obtaining non-trivial dynamics in residual networks, impacting performance for initialized and trained networks.

The residual scaling parameter affects the behavior of gradients in ResNets: Smaller scaling values reduce the whitening of gradients with increasing depth [37]. Zaemzadeh *et al.* [38] show that skip connections lead to norm-preservation of the gradients during backpropagation by shifting the singular values closer to one; norm-preservation in turn improves trainability and generalization. Regarding the problem of vanishing or exploding gradients, Ling and Qiu [39] require the singular values of the input-output Jacobian to be of order one, suggesting a scaling of the weight variance by the square root of the inverse depth. While their result holds only in the double limit of infinite width and depth, our theoretical predictions apply to finite-size networks.

Another line of research studies the scaling of the skip connection instead of the residual branch: According to Zhang *et al.* [40], scaling the skip connection improves semantic feature learning; suggesting an inverse scaling with depth while observing that the particular decay scheme is less relevant than the total decay over all layers. Doshi *et al.* [41] investigate critical points in residual networks, observing only a weak dependence on other hyperparameters such as weight and bias variance at initialization similar as the weak dependence explained by the here-developed theory; they empirically compute partial Jacobians while we study the response function that naturally appears in the presented field-theoretic framework. Scaling the skip connections can straightforwardly be included into this framework; we leave this for future work.

Outlook The field-theoretic formulation in Section II allows the systematic computation of finite-size corrections to the NNGP result. Fischer *et al.* [42] compute the

Bayesian posterior network kernel that results from fluctuation corrections to the NNGP kernels in feed-forward networks. In the future, we plan to investigate the effect of skip connections on the network posterior in this framework. Further, Lindner *et al.* [43] employ a related framework for studying the effect of data variability on the network posterior, which is also an interesting avenue of future research for residual networks.

ACKNOWLEDGMENTS

We thank Peter Bouss and Claudia Merger for helpful discussions. This work was partly supported by the

German Federal Ministry for Education and Research (BMBF Grant 01IS19077A to Jülich and BMBF Grant 01IS19077B to Aachen) and funded by the Deutsche Forschungsgemeinschaft (DFG, German Research Foundation) - 368482240/GRK2416, the Excellence Initiative of the German federal and state governments (ERS PF-JARA-SDS005), and the Helmholtz Association Initiative and Networking Fund under project number SO-092 (Advanced Computing Architectures, ACA). Open access publication funded by the Deutsche Forschungsgemeinschaft (DFG, German Research Foundation) - 491111487.

Appendix A NETWORK PRIOR FOR MULTIPLE INPUTS

We calculate the network prior $p(Y|X)$ as derived in Section II for multiple inputs $X = (x_\alpha)_{\alpha=1,\dots,P}$ and network outputs $Y = (y_\alpha)_{\alpha=1,\dots,P}$:

$$p(Y|X) = \int d\theta \prod_{\alpha} p(y_\alpha|x_\alpha, \theta) p(\theta). \quad (26)$$

For fixed network parameters θ , the probability $p(Y|X, \theta)$ is given by enforcing the network model with Dirac δ -distributions as

$$\begin{aligned} p(Y|X, \theta) = & \prod_{\alpha} \int dh_{\alpha}^{(0)} \dots \int dh_{\alpha}^{(L)} \delta(h_{\alpha}^{(0)} - W^{\text{in}} x_{\alpha} - b^{\text{in}}) \\ & \times \prod_{l=1}^L \delta(h_{\alpha}^{(l)} - h_{\alpha}^{(l-1)} - \rho W^{(l)} \phi(h_{\alpha}^{(l-1)}) - \rho b^{(l)}) \\ & \times \delta(y_{\alpha} - W^{\text{out}} \phi(h_{\alpha}^{(L)}) - b^{\text{out}}). \end{aligned} \quad (27)$$

Marginalization over network parameters

We marginalize over network parameters

$$\begin{aligned} p(Y|X) = & \prod_{\alpha} \int dh_{\alpha}^{(0)} \dots \int dh_{\alpha}^{(L)} \langle \delta(h_{\alpha}^{(0)} - W^{\text{in}} x_{\alpha} - b^{\text{in}}) \rangle_{\{W^{\text{in}}, b^{\text{in}}\}} \\ & \times \prod_{l=1}^L \langle \delta(h_{\alpha}^{(l)} - h_{\alpha}^{(l-1)} - \rho W^{(l)} \phi(h_{\alpha}^{(l-1)}) - \rho b^{(l)}) \rangle_{\{W^{(l)}, b^{(l)}\}} \\ & \times \langle \delta(y_{\alpha} - W^{\text{out}} \phi(h_{\alpha}^{(L)}) - b^{\text{out}}) \rangle_{\{W^{\text{out}}, b^{\text{out}}\}}, \end{aligned} \quad (28)$$

where $\langle \dots \rangle_{\{W, b\}}$ refers to the Gaussian average over weights W and biases b . Using the Fourier representation $\delta(h) = \int d\tilde{h} \exp(\tilde{h}^T h)$ of the Dirac Delta distribution with $\tilde{h}^T h = \sum_{i=1}^N \tilde{h}_i h_i$, integration measure $\int d\tilde{h} = \prod_k \int_{i\mathbb{R}} \frac{d\tilde{h}_k}{2\pi i}$ and \tilde{h} the conjugate variable to h , we have

$$\begin{aligned} p(Y|X) = & \prod_{\alpha} \left\{ \int \mathcal{D}\tilde{y}_{\alpha} \int \mathcal{D}\tilde{h}_{\alpha} \int \mathcal{D}h_{\alpha} \right\} \left\langle \exp \left(\sum_{\alpha, i} \tilde{h}_{i, \alpha}^{(0)} (h_{i, \alpha}^{(0)} - \sum_j W_{ij}^{\text{in}} x_{j, \alpha} - b_i^{\text{in}}) \right) \right\rangle_{\{W^{\text{in}}, b^{\text{in}}\}} \\ & \times \prod_{l=1}^L \left\langle \exp \left(\sum_{\alpha, i} \tilde{h}_{i, \alpha}^{(l)} (h_{i, \alpha}^{(l)} - h_{i, \alpha}^{(l-1)} - \rho \sum_j W_{ij}^{(l)} \phi_{j, \alpha}^{(l-1)} - \rho b_i^{(l)}) \right) \right\rangle_{\{W^{(l)}, b^{(l)}\}} \\ & \times \left\langle \exp \left(\sum_{\alpha, i} \tilde{y}_{i, \alpha} (y_{i, \alpha} - \sum_j W_{ij}^{\text{out}} \phi_{j, \alpha}^{(L)} - b_i^{\text{out}}) \right) \right\rangle_{\{W^{\text{out}}, b^{\text{out}}\}}, \end{aligned} \quad (29)$$

where $\int \mathcal{D}h_\alpha = \prod_{l=0}^L \int dh_\alpha^{(l)}$ and $\int \mathcal{D}\tilde{h}_\alpha = \prod_{l=0}^L \int d\tilde{h}_\alpha^{(l)}$. We introduced the shorthand $\phi_{j,\alpha}^{(l-1)} = \phi(h_{j,\alpha}^{(l-1)})$ for brevity. Since the network parameters θ are independently distributed, we can compute the averages for each parameter separately $\int d\theta_k p(\theta_k) \exp(z\theta_k)$, which yields the moment-generating function of the distribution $p(\theta_k)$. For Gaussian distributed parameters $\theta_k \sim \mathcal{N}(0, \sigma^2)$, this gives $\exp(\frac{1}{2}\sigma^2 z^2)$. For the individual terms in Eq. (29), we get

$$\begin{aligned}
\left\langle \exp\left(-\sum_{i,j} W_{ij}^{\text{in}} \sum_{\alpha} \tilde{h}_{i,\alpha}^{(0)} x_{j,\alpha}\right) \right\rangle_{W^{\text{in}}} &= \exp\left(\frac{1}{2} \frac{\sigma_{w,\text{in}}^2}{d_{\text{in}}} \sum_{i,j} \left(\sum_{\alpha} \tilde{h}_{i,\alpha}^{(0)} x_{j,\alpha}\right)^2\right) \\
&= \exp\left(\frac{1}{2} \frac{\sigma_{w,\text{in}}^2}{d_{\text{in}}} \sum_{\alpha,\beta} \sum_{i,j} \tilde{h}_{i,\alpha}^{(0)} x_{j,\alpha} \tilde{h}_{i,\beta}^{(0)} x_{j,\beta}\right), \\
\left\langle \exp\left(-\sum_i b_i^{\text{in}} \sum_{\alpha} \tilde{h}_{i,\alpha}^{(0)}\right) \right\rangle_{b^{\text{in}}} &= \exp\left(\frac{1}{2} \sigma_{b,\text{in}}^2 \sum_i \left(\sum_{\alpha} \tilde{h}_{i,\alpha}^{(0)}\right)^2\right) \\
&= \exp\left(\frac{1}{2} \sigma_{b,\text{in}}^2 \sum_{\alpha,\beta} \sum_i \tilde{h}_{i,\alpha}^{(0)} \tilde{h}_{i,\beta}^{(0)}\right), \\
\left\langle \exp\left(-\sum_{i,j} W_{ij}^{(l)} \rho \sum_{\alpha} \tilde{h}_{i,\alpha}^{(l)} \phi_{j,\alpha}^{(l-1)}\right) \right\rangle_{W^{(l)}} &= \exp\left(\frac{1}{2} \frac{\sigma_w^2}{N} \sum_{i,j} \left(\rho \sum_{\alpha} \tilde{h}_{i,\alpha}^{(l)} \phi_{j,\alpha}^{(l-1)}\right)^2\right) \\
&= \exp\left(\frac{1}{2} \rho^2 \frac{\sigma_w^2}{N} \sum_{\alpha,\beta} \sum_{i,j} \tilde{h}_{i,\alpha}^{(l)} \phi_{j,\alpha}^{(l-1)} \tilde{h}_{i,\beta}^{(l)} \phi_{j,\beta}^{(l-1)}\right), \\
\left\langle \exp\left(-\sum_i b_i^{(l)} \rho \sum_{\alpha} \tilde{h}_{i,\alpha}^{(l)}\right) \right\rangle_{b^{(l)}} &= \exp\left(\frac{1}{2} \sigma_b^2 \sum_i \left(\rho \sum_{\alpha} \tilde{h}_{i,\alpha}^{(l)}\right)^2\right) \\
&= \exp\left(\frac{1}{2} \rho^2 \sigma_b^2 \sum_{\alpha,\beta} \sum_i \tilde{h}_{i,\alpha}^{(l)} \tilde{h}_{i,\beta}^{(l)}\right), \\
\left\langle \exp\left(-\sum_{i,j} W_{ij}^{\text{out}} \sum_{\alpha} \tilde{y}_{i,\alpha} \phi_{j,\alpha}^{(L)}\right) \right\rangle_{W^{\text{out}}} &= \exp\left(\frac{1}{2} \frac{\sigma_{w,\text{out}}^2}{N} \sum_{i,j} \left(\sum_{\alpha} \tilde{y}_{i,\alpha} \phi_{j,\alpha}^{(L)}\right)^2\right) \\
&= \exp\left(\frac{1}{2} \frac{\sigma_{w,\text{out}}^2}{N} \sum_{\alpha,\beta} \sum_{i,j} \tilde{y}_{i,\alpha} \phi_{j,\alpha}^{(L)} \tilde{y}_{i,\beta} \phi_{j,\beta}^{(L)}\right), \\
\left\langle \exp\left(-\sum_i b_i^{\text{out}} \sum_{\alpha} \tilde{y}_{i,\alpha}\right) \right\rangle_{b^{\text{out}}} &= \exp\left(\frac{1}{2} \sigma_{b,\text{out}}^2 \sum_i \left(\sum_{\alpha} \tilde{y}_{i,\alpha}\right)^2\right) \\
&= \exp\left(\frac{1}{2} \sigma_{b,\text{out}}^2 \sum_{\alpha,\beta} \sum_i \tilde{y}_{i,\alpha} \tilde{y}_{i,\beta}\right).
\end{aligned}$$

To ease notation, we use an implicit summation convention in the following for lower indices that appear twice in the exponent, e.g. $\sum_{\alpha} \sum_i \tilde{h}_{i,\alpha}^{(l)} \tilde{h}_{i,\alpha}^{(l)} = \tilde{h}_{i,\alpha}^{(l)} \tilde{h}_{i,\alpha}^{(l)}$. Further, we write $\int \mathcal{D}h = \prod_{\alpha} \int \mathcal{D}h_{\alpha}$. Rewriting the sums over neuron indices, we overall get for the prior

$$\begin{aligned}
p(Y|X) &= \int \mathcal{D}\tilde{y} \int \mathcal{D}\tilde{h} \int \mathcal{D}h \exp\left(\tilde{y}_{\alpha}^{\text{T}} y_{\alpha} + \frac{1}{2} \frac{\sigma_{w,\text{out}}^2}{N} \tilde{y}_{\alpha}^{\text{T}} \tilde{y}_{\beta} [\phi_{\alpha}^{(L)}]^{\text{T}} \phi_{\beta}^{(L)} + \frac{1}{2} \sigma_{b,\text{out}}^2 \sum_{\alpha,\beta} \tilde{y}_{\alpha}^{\text{T}} \tilde{y}_{\beta}\right) \\
&\quad \times \exp\left(\sum_{l=1}^L [\tilde{h}_{\alpha}^{(l)}]^{\text{T}} [h_{\alpha}^{(l)} - h_{\alpha}^{(l-1)}]\right) \\
&\quad \times \exp\left(\sum_{l=1}^L \left(\frac{1}{2} \rho^2 \frac{\sigma_w^2}{N} [\tilde{h}_{\alpha}^{(l)}]^{\text{T}} \tilde{h}_{\beta}^{(l)} [\phi_{\alpha}^{(l-1)}]^{\text{T}} \phi_{\beta}^{(l-1)} + \frac{1}{2} \rho^2 \sigma_b^2 \sum_{\alpha,\beta} [\tilde{h}_{\alpha}^{(l)}]^{\text{T}} \tilde{h}_{\beta}^{(l)}\right)\right) \\
&\quad \times \exp\left([\tilde{h}_{\alpha}^{(0)}]^{\text{T}} h_{\alpha}^{(0)} + \frac{1}{2} \frac{\sigma_{w,\text{in}}^2}{d_{\text{in}}} [\tilde{h}_{\alpha}^{(0)}]^{\text{T}} \tilde{h}_{\beta}^{(0)} x_{\alpha}^{\text{T}} x_{\beta} + \frac{1}{2} \sigma_{b,\text{in}}^2 \sum_{\alpha,\beta} [\tilde{h}_{\alpha}^{(0)}]^{\text{T}} \tilde{h}_{\beta}^{(0)}\right) \\
&=: \int \mathcal{D}\tilde{y} \int \mathcal{D}\tilde{h} \int \mathcal{D}h \exp(\mathcal{S}(Y, \tilde{Y}, H, \tilde{H}|X)).
\end{aligned} \tag{30}$$

The action \mathcal{S} consists of three contributions

$$\mathcal{S}(Y, \tilde{Y}, H, \tilde{H}|X) = \mathcal{S}_{\text{in}}(H^{(0)}, \tilde{H}^{(0)}|X) + \mathcal{S}_{\text{net}}(H, \tilde{H}) + \mathcal{S}_{\text{out}}(Y, \tilde{Y}|H^{(L)}), \tag{31}$$

one term from the readin layer containing the dependence on the inputs X as

$$\mathcal{S}_{\text{in}}(H^{(0)}, \tilde{H}^{(0)}|X) := [\tilde{h}_\alpha^{(0)}]^\top h_\alpha^{(0)} + \frac{1}{2} \frac{\sigma_{w,\text{in}}^2}{d_{\text{in}}} [\tilde{h}_\alpha^{(0)}]^\top \tilde{h}_\beta^{(0)} x_\alpha^\top x_\beta + \frac{1}{2} \sigma_{b,\text{in}}^2 \sum_{\alpha,\beta} [\tilde{h}_\alpha^{(0)}]^\top \tilde{h}_\beta^{(0)}, \quad (32)$$

one term from the intermediate layers containing the skip connections

$$\mathcal{S}_{\text{net}}(H, \tilde{H}) := \sum_{l=1}^L [\tilde{h}_\alpha^{(l)}]^\top [h_\alpha^{(l)} - h_\alpha^{(l-1)}] + \frac{1}{2} \rho^2 \frac{\sigma_w^2}{N} [\tilde{h}_\alpha^{(l)}]^\top \tilde{h}_\beta^{(l)} [\phi_\alpha^{(l-1)}]^\top \phi_\beta^{(l-1)} + \frac{1}{2} \rho^2 \sigma_b^2 \sum_{\alpha,\beta} [\tilde{h}_\alpha^{(l)}]^\top \tilde{h}_\beta^{(l)}, \quad (33)$$

and one term for the readout layer containing the network outputs Y as

$$\mathcal{S}_{\text{out}}(Y, \tilde{Y}|H^{(L)}) := \tilde{y}_\alpha^\top y_\alpha + \frac{1}{2} \frac{\sigma_{w,\text{out}}^2}{N} \tilde{y}_\alpha^\top \tilde{y}_\beta [\phi_\alpha^{(L)}]^\top \phi_\beta^{(L)} + \frac{1}{2} \sigma_{b,\text{out}}^2 \tilde{y}_\alpha^\top \tilde{y}_\beta. \quad (34)$$

Auxiliary variables

To treat terms $\propto [\tilde{h}^{(l)}]^\top \tilde{h}^{(l)} \phi^{(l-1)\top} \phi^{(l-1)}$ that cannot be solved in general, we introduce auxiliary variables

$$C_{\alpha\beta}^{(l)} := \begin{cases} \frac{\sigma_{w,\text{in}}^2}{d_{\text{in},2}} (XX^\top)_{\alpha\beta} + \sigma_{b,\text{in}}^2 & l = 0, \\ \rho^2 \frac{\sigma_w^2}{N} \phi_\alpha^{(l-1)} \cdot \phi_\beta^{(l-1)} + \rho^2 \sigma_b^2 & 1 \leq l \leq L, \\ \frac{\sigma_{w,\text{out}}^2}{N} \phi_\alpha^{(L)} \cdot \phi_\beta^{(L)} + \sigma_{b,\text{out}}^2 & l = L+1, \end{cases} \quad (35)$$

which decouple these two terms. To account for the original interaction between \tilde{h} and $\phi^{(l-1)}$, we enforce the definition of the auxiliary variables by Dirac δ -distributions and obtain for the network prior

$$\begin{aligned} p(Y|X) = & \int \mathcal{D}\tilde{y} \int \mathcal{D}\tilde{h} \int \mathcal{D}h \prod_{\alpha,\beta} \int \mathcal{D}C_{\alpha\beta} \exp \left(\tilde{y}_\alpha^\top y_\alpha + \frac{1}{2} C_{\alpha\beta}^{(L+1)} \tilde{y}_\alpha^\top \tilde{y}_\beta \right) \delta \left(C_{\alpha\beta}^{(L+1)} - \frac{\sigma_{w,\text{out}}^2}{N} [\phi_\alpha^{(L)}]^\top \phi_\beta^{(L)} - \sigma_{b,\text{out}}^2 \right) \\ & \times \exp \left(\sum_{l=1}^L \left[[\tilde{h}_\alpha^{(l)}]^\top [h_\alpha^{(l)} - h_\alpha^{(l-1)}] + \frac{1}{2} C_{\alpha\beta}^{(l)} [\tilde{h}_\alpha^{(l)}]^\top \tilde{h}_\beta^{(l)} \right] \right) \delta \left(C_{\alpha\beta}^{(l)} - \rho^2 \frac{\sigma_w^2}{N} [\phi_\alpha^{(l-1)}]^\top \phi_\beta^{(l-1)} - \rho^2 \sigma_b^2 \right) \\ & \times \exp \left([\tilde{h}_\alpha^{(0)}]^\top h_\alpha^{(0)} + \frac{1}{2} C_{\alpha\beta}^{(0)} [\tilde{h}_\alpha^{(0)}]^\top \tilde{h}_\beta^{(0)} \right) \delta \left(C_{\alpha\beta}^{(0)} - \frac{\sigma_{w,\text{in}}^2}{d_{\text{in}}} x_\alpha \cdot x_\beta - \sigma_{b,\text{in}}^2 \right), \end{aligned}$$

with $\int \mathcal{D}C_{\alpha\beta} = \prod_{l=0}^{L+1} \int \mathcal{D}C_{\alpha\beta}^{(l)}$. We rewrite the Dirac δ -distributions using their Fourier representation $\delta(C_{\alpha\beta}^{(l)}) = \int_{i\mathbb{R}} \frac{d\tilde{C}_{\alpha\beta}^{(l)}}{2\pi i} \exp(\tilde{C}_{\alpha\beta}^{(l)} C_{\alpha\beta}^{(l)})$, introducing conjugate variables $\tilde{C}_{\alpha\beta}^{(l)}$ to the auxiliary variables $C_{\alpha\beta}^{(l)}$, as

$$\begin{aligned} \delta \left(d_{\text{in}} C_{\alpha\beta}^{(0)} - \sigma_{w,\text{in}}^2 x_\alpha \cdot x_\beta - d_{\text{in}} \sigma_{b,\text{in}}^2 \right) &= \int_{i\mathbb{R}} \frac{d\tilde{C}_{\alpha\beta}^{(0)}}{2\pi i} \exp \left(d_{\text{in}} \tilde{C}_{\alpha\beta}^{(0)} C_{\alpha\beta}^{(0)} - \sigma_{w,\text{in}}^2 \tilde{C}_{\alpha\beta}^{(0)} x_\alpha \cdot x_\beta - d_{\text{in}} \sigma_{b,\text{in}}^2 \tilde{C}_{\alpha\beta}^{(0)} \right), \\ \delta \left(N C_{\alpha\beta}^{(l)} - \rho^2 \sigma_w^2 [\phi_\alpha^{(l-1)}]^\top \phi_\beta^{(l-1)} - N \rho^2 \sigma_b^2 \right) &= \int_{i\mathbb{R}} \frac{d\tilde{C}_{\alpha\beta}^{(l)}}{2\pi i} \exp \left(N \tilde{C}_{\alpha\beta}^{(l)} C_{\alpha\beta}^{(l)} - \rho^2 \sigma_w^2 \tilde{C}_{\alpha\beta}^{(l)} [\phi_\alpha^{(l-1)}]^\top \phi_\beta^{(l-1)} - N \rho^2 \sigma_b^2 \tilde{C}_{\alpha\beta}^{(l)} \right), \\ \delta \left(N C_{\alpha\beta}^{(L+1)} - \sigma_{w,\text{out}}^2 [\phi_\alpha^{(L)}]^\top \phi_\beta^{(L)} - N \sigma_{b,\text{out}}^2 \right) &= \int_{i\mathbb{R}} \frac{d\tilde{C}_{\alpha\beta}^{(L+1)}}{2\pi i} \exp \left(N \tilde{C}_{\alpha\beta}^{(L+1)} C_{\alpha\beta}^{(L+1)} - \sigma_{w,\text{out}}^2 \tilde{C}_{\alpha\beta}^{(L+1)} [\phi_\alpha^{(L)}]^\top \phi_\beta^{(L)} - N \sigma_{b,\text{out}}^2 \tilde{C}_{\alpha\beta}^{(L+1)} \right). \end{aligned}$$

Altogether, we obtain

$$\begin{aligned}
p(Y|X) = & \int \mathcal{D}\tilde{y} \int \mathcal{D}\tilde{h} \int \mathcal{D}h \int \mathcal{D}C \int \mathcal{D}\tilde{C} \exp \left(\tilde{y}_\alpha^\top y_\alpha + \frac{1}{2} C_{\alpha\beta}^{(L+1)} \tilde{y}_\alpha^\top \tilde{y}_\beta \right) \\
& \times \exp \left(\sum_{l=1}^L \left[[\tilde{h}_\alpha^{(l)}]^\top [h_\alpha^{(l)} - h_\alpha^{(l-1)}] + \frac{1}{2} C_{\alpha\beta}^{(l)} [\tilde{h}_\alpha^{(l)}]^\top \tilde{h}_\beta^{(l)} \right] \right) \\
& \times \exp \left([\tilde{h}_\alpha^{(0)}]^\top h_\alpha^{(0)} + \frac{1}{2} C_{\alpha\beta}^{(0)} [\tilde{h}_\alpha^{(0)}]^\top \tilde{h}_\beta^{(0)} \right) \\
& \times \exp \left(-N \sum_{l=0}^{L+1} \nu_l C_{\alpha\beta}^{(l)} \tilde{C}_{\alpha\beta}^{(l)} + \rho^2 \sigma_w^2 \sum_{l=1}^L \tilde{C}_{\alpha\beta}^{(l)} [\phi_\alpha^{(l-1)}]^\top \phi_\beta^{(l-1)} + N \rho^2 \sigma_b^2 \sum_{l=1}^L \sum_{\alpha,\beta} \tilde{C}_{\alpha\beta}^{(l)} \right) \\
& \times \exp \left(\sigma_{w,\text{out}}^2 \tilde{C}_{\alpha\beta}^{(L+1)} [\phi_\alpha^{(L)}]^\top \phi_\beta^{(L)} + N \sigma_{b,\text{out}}^2 \sum_{\alpha,\beta} \tilde{C}_{\alpha\beta}^{(L+1)} \right) \\
& \times \exp \left(\sigma_{w,\text{in}}^2 \tilde{C}_{\alpha\beta}^{(0)} (XX^\top)_{\alpha\beta} + d_{\text{in}} \sigma_{b,\text{in}}^2 \sum_{\alpha,\beta} \tilde{C}_{\alpha\beta}^{(0)} \right),
\end{aligned}$$

where we write $\int \mathcal{D}C = \prod_{\alpha,\beta} \{\int \mathcal{D}C_{\alpha\beta}\}$ and $\int \mathcal{D}\tilde{C} = \prod_{\alpha,\beta} \prod_{l=0}^{L+1} \int_{i\mathbb{R}} \frac{d\tilde{C}_{\alpha\beta}^{(l)}}{2\pi i}$ and $\nu_l = 1 + \delta_{0l} (d_{\text{in}}/N - 1)$. The scalar variables $C_{\alpha\beta}^{(l)}$ and $\tilde{C}_{\alpha\beta}^{(l)}$ only couple to sums of $\tilde{h}^{(l)}$ and $\phi^{(l)}$ over all neuron indices, so all components of $h^{(l)}$ and $\tilde{h}^{(l)}$ are identically distributed. We can thus rewrite

$$\begin{aligned}
p(Y|X) = & \int \mathcal{D}\tilde{y} \int \mathcal{D}\tilde{h} \int \mathcal{D}h \int \mathcal{D}C \int \mathcal{D}\tilde{C} \exp \left(\tilde{y}_\alpha^\top y_\alpha + \frac{1}{2} C_{\alpha\beta}^{(L+1)} \tilde{y}_\alpha^\top \tilde{y}_\beta \right) \\
& \times \exp \left(N \sum_{l=1}^L \left[\tilde{h}_\alpha^{(l)} [h_\alpha^{(l)} - h_\alpha^{(l-1)}] + \frac{1}{2} \tilde{h}_\alpha^{(l)} C_{\alpha\beta}^{(l)} \tilde{h}_\beta^{(l)} \right] \right) \\
& \times \exp \left(N \sum_{\alpha} \tilde{h}_\alpha^{(0)} h_\alpha^{(0)} + N \frac{1}{2} \sum_{\alpha,\beta} \tilde{h}_\alpha^{(0)} C_{\alpha\beta}^{(0)} \tilde{h}_\beta^{(0)} \right) \\
& \times \exp \left(-N \sum_{l=0}^{L+1} \nu_l C_{\alpha\beta}^{(l)} \tilde{C}_{\alpha\beta}^{(l)} + N \rho^2 \sigma_w^2 \sum_{l=1}^L \phi_\alpha^{(l-1)} \tilde{C}_{\alpha\beta}^{(l)} \phi_\beta^{(l-1)} + N \rho^2 \sigma_b^2 \sum_{l=1}^L \sum_{\alpha,\beta} \tilde{C}_{\alpha\beta}^{(l)} \right) \\
& \times \exp \left(N \sigma_{w,\text{out}}^2 \phi_\alpha^{(L)} \tilde{C}_{\alpha\beta}^{(L+1)} \phi_\beta^{(L)} + N \sigma_{b,\text{out}}^2 \sum_{\alpha,\beta} \tilde{C}_{\alpha\beta}^{(L+1)} \right) \\
& \times \exp \left(\sigma_{w,\text{in}}^2 \tilde{C}_{\alpha\beta}^{(0)} (XX^\top)_{\alpha\beta} + d_{\text{in}} \sigma_{b,\text{in}}^2 \sum_{\alpha,\beta} \tilde{C}_{\alpha\beta}^{(0)} \right).
\end{aligned}$$

Now $h^{(l)}$ and $\tilde{h}^{(l)}$ refer to scalar quantities. To get a formulation in terms of the order parameters $C_{\alpha\beta}^{(l)}$, we move the integrals over $h^{(l)}$ and $\tilde{h}^{(l)}$ into the exponent, yielding

$$\begin{aligned}
p(Y|X) &= \int \mathcal{D}\tilde{y} \int \mathcal{D}C \int \mathcal{D}\tilde{C} \exp \left(\tilde{y}_\alpha^\top y_\alpha + \frac{1}{2} C_{\alpha\beta}^{(L+1)} \tilde{y}_\alpha^\top \tilde{y}_\beta - N \sum_{l=0}^{L+1} \nu_l C_{\alpha\beta}^{(l)} \tilde{C}_{\alpha\beta}^{(l)} \right) \\
&\quad \times \exp \left[N \ln \prod_{l=1}^L \int \mathcal{D}\tilde{h}^{(l)} \int \mathcal{D}h^{(l)} \exp \left(\tilde{h}_\alpha^{(l)} [h_\alpha^{(l)} - h_\alpha^{(l-1)}] + \frac{1}{2} \tilde{h}_\alpha^{(l)} C_{\alpha\beta}^{(l)} \tilde{h}_\beta^{(l)} \right) \right. \\
&\quad \times \exp \left(\rho^2 \sigma_w^2 \sum_{l=1}^L \phi_\alpha^{(l-1)} \tilde{C}_{\alpha\beta}^{(l)} \phi_\beta^{(l-1)} + \rho^2 \sigma_b^2 \sum_{l=1}^L \sum_{\alpha,\beta} \tilde{C}_{\alpha\beta}^{(l)} \right) \\
&\quad \times \exp \left(\sigma_{w,\text{out}}^2 \phi_\alpha^{(L)} \tilde{C}_{\alpha\beta}^{(L+1)} \phi_\beta^{(L)} + \sigma_{b,\text{out}}^2 \sum_{\alpha,\beta} \tilde{C}_{\alpha\beta}^{(L+1)} \right) \\
&\quad \times \int \mathcal{D}\tilde{h}^{(0)} \int \mathcal{D}h^{(0)} \exp \left(\tilde{h}_\alpha^{(0)} h_\alpha^{(0)} + \frac{1}{2} \tilde{h}_\alpha^{(0)} C_{\alpha\beta}^{(0)} \tilde{h}_\beta^{(0)} \right) \\
&\quad \left. \times \exp \left(\sigma_{w,\text{in}}^2 \tilde{C}_{\alpha\beta}^{(0)} (XX^\top)_{\alpha\beta} + d_{\text{in}} \sigma_{b,\text{in}}^2 \sum_{\alpha,\beta} \tilde{C}_{\alpha\beta}^{(0)} \right) \right] \\
&= \int \mathcal{D}\tilde{y} \left\langle \exp \left(\tilde{y}_\alpha^\top y_\alpha + \frac{1}{2} \tilde{y}_\alpha^\top C_{\alpha\beta}^{(L+1)} \tilde{y}_\beta \right) \right\rangle_{C, \tilde{C}}.
\end{aligned}$$

The expectation value appearing in the last line is with respect to the auxiliary variable and its conjugate variable, which are distributed according to the auxiliary action $(C, \tilde{C}) \sim \exp(S(C, \tilde{C}))$ given by

$$\begin{aligned}
\mathcal{S}(C, \tilde{C}) &:= -N \sum_{l=0}^{L+1} \nu_l C_{\alpha\beta}^{(l)} \tilde{C}_{\alpha\beta}^{(l)} + N \mathcal{W}(\tilde{C}|C), \\
\mathcal{W}(\tilde{C}|C) &:= \ln \prod_{l=1}^L \int \mathcal{D}\tilde{h}^{(l)} \int \mathcal{D}h^{(l)} \exp \left(\tilde{h}_\alpha^{(l)} [h_\alpha^{(l)} - h_\alpha^{(l-1)}] + \frac{1}{2} \tilde{h}_\alpha^{(l)} C_{\alpha\beta}^{(l)} \tilde{h}_\beta^{(l)} \right) \\
&\quad \times \exp \left(\rho^2 \sigma_w^2 \sum_{l=1}^L \phi_\alpha^{(l-1)} \tilde{C}_{\alpha\beta}^{(l)} \phi_\beta^{(l-1)} + \rho^2 \sigma_b^2 \sum_{l=1}^L \sum_{\alpha,\beta} \tilde{C}_{\alpha\beta}^{(l)} \right) \\
&\quad \times \exp \left(\sigma_{w,\text{out}}^2 \phi_\alpha^{(L)} \tilde{C}_{\alpha\beta}^{(L+1)} \phi_\beta^{(L)} + \sigma_{b,\text{out}}^2 \sum_{\alpha,\beta} \tilde{C}_{\alpha\beta}^{(L+1)} \right) \\
&\quad \times \int \mathcal{D}\tilde{h}^{(0)} \int \mathcal{D}h^{(0)} \exp \left(N \tilde{h}_\alpha^{(0)} h_\alpha^{(0)} + N \frac{1}{2} \tilde{h}_\alpha^{(0)} C_{\alpha\beta}^{(0)} \tilde{h}_\beta^{(0)} + \sigma_{w,\text{in}}^2 \tilde{C}_{\alpha\beta}^{(0)} (XX^\top)_{\alpha\beta} + d_{\text{in}} \sigma_{b,\text{in}}^2 \sum_{\alpha,\beta} \tilde{C}_{\alpha\beta}^{(0)} \right).
\end{aligned}$$

Saddle point approximation

Since the action \mathcal{S} scales with the network width N , we can perform a saddle point approximation for infinite width $N \rightarrow \infty$. We compute the saddle points C_* , \tilde{C}_* using the conditions

$$\frac{\partial \mathcal{S}}{\partial C_{\alpha\beta}^{(l)}} \stackrel{!}{=} 0, \quad \frac{\partial \mathcal{S}}{\partial \tilde{C}_{\alpha\beta}^{(l)}} \stackrel{!}{=} 0,$$

and obtain

$$\begin{aligned}
C_{\alpha\beta,*}^{(l)} &= \begin{cases} \frac{\sigma_{w,\text{in}}^2}{d_{\text{in}}} (XX^\top)_{\alpha\beta} + \sigma_{b,\text{in}}^2 & l = 0, \\ \rho^2 \sigma_w^2 \langle \phi_\alpha^{(l-1)} \phi_\beta^{(l-1)} \rangle_p + \rho^2 \sigma_b^2 & 1 \leq l \leq L, \\ \sigma_{w,\text{out}}^2 \langle \phi_\alpha^{(L)} \phi_\beta^{(L)} \rangle_p + \sigma_{b,\text{out}}^2 & l = L+1, \end{cases} \\
\tilde{C}_*^{(l)} &= 0 \quad l = 0, \dots, L+1,
\end{aligned}$$

where

$$\begin{aligned} \langle \dots \rangle_p = & \prod_{l=1}^L \int \mathcal{D}\tilde{h}^{(l)} \int \mathcal{D}h^{(l)} \dots \exp \left(\tilde{h}_\alpha^{(l)} [h_\alpha^{(l)} - h_\alpha^{(l-1)}] + \frac{1}{2} \tilde{h}_\alpha^{(l)} C_{\alpha\beta,*}^{(l)} \tilde{h}_\beta^{(l)} \right) \\ & \times \int \mathcal{D}\tilde{h}^{(0)} \int \mathcal{D}h^{(0)} \exp \left(\tilde{h}_\alpha^{(0)} h_\alpha^{(0)} + \frac{1}{2} \tilde{h}_\alpha^{(0)} C_{\alpha\beta,*}^{(0)} \tilde{h}_\beta^{(0)} \right). \end{aligned}$$

While the input kernel $C^0 = C_*^0$ is fixed, all other residual kernels C_*^l are computed self-consistently with respect to the expectation value involving C_*^l . We can rewrite this average by using the defining residual $f^{(l)} = h^{(l)} - h^{(l-1)}$ for $1 \leq l \leq L$ and get

$$\begin{aligned} \langle \dots \rangle_p = & \int \mathcal{D}h^{(0)} \int \mathcal{D}\tilde{h}^{(0)} \exp \left(\tilde{h}_\alpha^{(0)} h_\alpha^{(0)} + \frac{1}{2} \tilde{h}_\alpha^{(0)} C_{\alpha\beta,*}^{(0)} \tilde{h}_\beta^{(0)} \right) \\ & \times \prod_{l=1}^L \int \mathcal{D}f^{(l)} \int \mathcal{D}\tilde{h}^{(l)} \dots \exp \left(\tilde{h}_\alpha^{(l)} f_\alpha^{(l)} + \frac{1}{2} \tilde{h}_\alpha^{(l)} C_{\alpha\beta,*}^{(l)} \tilde{h}_\beta^{(l)} \right) \end{aligned} \quad (36)$$

$$= \int \mathcal{D}h^{(0)} \mathcal{N}(h^{(0)}|0, C_{\alpha\beta,*}^{(0)}) \prod_{l=1}^L \int \mathcal{D}f^{(l)} \dots \mathcal{N}(f^{(l)}|0, C_{\alpha\beta,*}^{(l)}), \quad (37)$$

where $\mathcal{N}(f^{(l)}|0, C_{\alpha\beta,*}^{(l)})$ denotes a multi-dimensional Gaussian with zero mean and covariance $C_{\alpha\beta,*}^{(l)}$. It follows that the input signal $H^{(0)} = (h_\alpha^{(0)})_{\alpha=1,\dots,P}$ is Gaussian distributed with zero mean and covariance matrix $C_{\alpha\beta,*}^{(0)}$ and the residuals $F^{(l)} = (f_\alpha^{(l)})_{\alpha=1,\dots,P}$ are Gaussian distributed with zero mean and covariance matrix $C_{\alpha\beta,*}^{(l)}$. The signal $h^{(l)}$ decomposes into a sum of the residuals as $h^{(l)} = h^{(0)} + \sum_{k=1}^l f^{(k)}$. Since the residuals $f^{(l)}$ are independent Gaussians and means and covariances for independent Gaussians sum up, the signal $h^{(l)}$ is also Gaussian distributed with covariance $K^{(l)} = \sum_{k=0}^l C_*^{(k)}$. Using the recursion relation $K^{(l)} = K^{(l-1)} + C_*^{(l-1)}$, we recover the NNGP result [8, 10, 11] for residual networks

$$C_{\alpha\beta,*}^{(l)} = \rho^2 \sigma_w^2 \langle \phi_\alpha^{(l-1)} \phi_\beta^{(l-1)} \rangle_{\mathcal{N}(0, K^{(l-1)})} + \rho^2 \sigma_b^2, \text{ for } 1 \leq l \leq L, \quad (38)$$

$$K_{\alpha\beta}^{(l)} = \begin{cases} \frac{\sigma_{w,\text{in}}^2}{d_{\text{in}}} (XX^\top)_{\alpha\beta} + \sigma_{b,\text{in}}^2 & l = 0, \\ K_{\alpha\beta}^{(l-1)} + C_{\alpha\beta,*}^{(l-1)} & 1 \leq l \leq L, \\ \sigma_{w,\text{out}}^2 \langle \phi_\alpha^{(L)} \phi_\beta^{(L)} \rangle_{\mathcal{N}(0, K^{(L)})} + \sigma_{b,\text{out}}^2 & l = L + 1. \end{cases} \quad (39)$$

Appendix B NEXT-TO-LEADING-ORDER CORRECTIONS

We compute the next-to-leading-order corrections to the saddle points in the previous section. While the auxiliary variables $C^{(l)}$ concentrate to the saddle point $C_*^{(l)}$ for infinite width $N \rightarrow \infty$, they fluctuate around this value for large but finite network width N . To lowest order, these fluctuations are Gaussian and can be obtained by computing the Hessian of the action \mathcal{S} at the saddle point

$$\begin{aligned} p(Y|X) & \simeq \int \mathcal{D}\delta C \int \mathcal{D}\delta\tilde{C} \exp \left(\frac{1}{2} (\delta C, \delta\tilde{C})^\top \mathcal{S}^{(2)} (\delta C, \delta\tilde{C}) \right) \\ & = \int \mathcal{D}\delta C \int \mathcal{D}\delta\tilde{C} \exp \left(-\frac{1}{2} (\delta C, \delta\tilde{C})^\top \Delta^{(2)} (\delta C, \delta\tilde{C}) \right), \end{aligned}$$

where we write $\delta C = C - C^*$, $\delta\tilde{C} = \tilde{C} - \tilde{C}^*$ and the negative inverse of the Hessian corresponds to their covariance

$$\Delta = -(\mathcal{S}^{(2)})^{-1} =: \begin{pmatrix} \langle \delta C \delta C \rangle & \langle \delta C \delta\tilde{C} \rangle \\ \langle \delta\tilde{C} \delta C \rangle & \langle \delta\tilde{C} \delta\tilde{C} \rangle \end{pmatrix}.$$

We evaluate all terms at the saddle point; thus there is no linear term and all expectation values that appear in the following are with respect to the Gaussian measure $\langle \dots \rangle_p$ in Eq. (36).

The diagonal entries of the Hessian are given by

$$\frac{\partial^2}{\partial C_{\alpha\beta}^{(l)} \partial C_{\gamma\beta}^{(k)}} \mathcal{S}|_{(C_*, \tilde{C}_*)} = 0, \quad (40)$$

$$\begin{aligned} \frac{\partial^2}{\partial \tilde{C}_{\alpha\beta}^{(l)} \partial \tilde{C}_{\gamma\delta}^{(k)}} \mathcal{S}|_{(C_*, \tilde{C}_*)} &= \frac{\partial}{\partial \tilde{C}_{\alpha\beta}^{(l)}} \left(N[\delta_{k,L+1} + (1 - \delta_{k,L+1})\rho^2] \sigma_w^2 \langle \phi_\gamma^{(k-1)} \phi_\delta^{(k-1)} \rangle_p + \text{const.}(\tilde{C}) \right) \\ &= \delta_{L0} N [\sigma_{w,\text{in}}^2 (XX^\top)_{\alpha\beta} + d_{\text{in}}] [\delta_{k,L+1} + (1 - \delta_{k,L+1})\rho^2] \sigma_w^2 \langle \phi_\gamma^{(k-1)} \phi_\delta^{(k-1)} \rangle_p \\ &\quad + N \sigma_w^4 1_{l>0} 1_{k>0} \langle \phi_\alpha^{(l-1)} \phi_\beta^{(l-1)}, \phi_\gamma^{(k-1)} \phi_\delta^{(k-1)} \rangle_p^c \\ &\quad \times \begin{cases} \rho^4 & k, l \neq L+1, \\ \rho^2 & k \neq l = L+1 \vee l \neq k = L+1, \\ 1 & \text{else,} \end{cases} \end{aligned} \quad (41)$$

where $1_{l>0}$ denotes the indicator function. We write $\langle \dots \rangle^c$ for connected correlations defined as

$$\langle \phi_\alpha^{(l-1)} \phi_\beta^{(l-1)}, \phi_\gamma^{(k-1)} \phi_\delta^{(k-1)} \rangle_p^c = \langle \phi_\alpha^{(l-1)} \phi_\beta^{(l-1)} \phi_\gamma^{(k-1)} \phi_\delta^{(k-1)} \rangle_p - \langle \phi_\alpha^{(l-1)} \phi_\beta^{(l-1)} \rangle_p \langle \phi_\gamma^{(k-1)} \phi_\delta^{(k-1)} \rangle_p.$$

The off-diagonal terms compute to

$$\begin{aligned} &\frac{\partial^2}{\partial C_{\alpha\beta}^{(l)} \partial \tilde{C}_{\gamma\delta}^{(k)}} \mathcal{S}|_{(C_*, \tilde{C}_*)} \\ &= -N \nu_l \delta_{kl} + N 1_{k>0} \sigma_w^2 \frac{\partial}{\partial C_{\alpha\beta}^{(l)}} \langle \phi_\gamma^{(k-1)} \phi_\delta^{(k-1)} \rangle_p \times \begin{cases} \rho^2 & k \leq L \\ 1 & k = L+1 \end{cases} \\ &= -N \nu_l \delta_{kl} + N 1_{k>0} \sigma_w^2 \frac{\partial}{\partial K_{\alpha\beta}^{(k-1)}} \langle \phi_\gamma^{(k-1)} \phi_\delta^{(k-1)} \rangle_{\mathcal{N}(0, K^{(k-1)})} \frac{\partial}{\partial C_{\alpha\beta}^{(l)}} K_{\alpha\beta}^{(k-1)} \times \begin{cases} \rho^2 & k \leq L \\ 1 & k = L+1 \end{cases} \\ &= -N \nu_l \delta_{kl} + N \delta_{(\alpha\beta), (\gamma\delta)} 1_{k>0} \sigma_w^2 \left([\phi_\alpha^{(k-1)}]' [\phi_\beta^{(k-1)}]' + \delta_{\alpha\beta} [\phi_\alpha^{(k-1)}]'' [\phi_\beta^{(k-1)}]'' \right)_{\mathcal{N}(0, K^{(k-1)})} 1_{k>l} \times \begin{cases} \rho^2 & k \leq L \\ 1 & k = L+1 \end{cases} \end{aligned} \quad (42)$$

where we used Price's theorem [22, 44] from the third to fourth line. The condition $k > l$ enforced by the indicator function $1_{k>l}$ results from the term $\frac{\partial}{\partial C^{(l)}} K^{(k-1)}$, because the network kernel $K^{(k-1)}$ only depends on the residual kernels $C^{(l)}$ with $l < k$.

To calculate the negative inverse of the Hessian, we write

$$\mathcal{S}^{(2)} = \begin{pmatrix} \frac{\partial^2}{\partial C^2} \mathcal{S} & \frac{\partial^2}{\partial C \partial \tilde{C}} \mathcal{S} \\ \frac{\partial^2}{\partial \tilde{C} \partial C} \mathcal{S} & \frac{\partial^2}{\partial \tilde{C}^2} \mathcal{S} \end{pmatrix} =: \begin{pmatrix} \mathcal{S}_{11} & \mathcal{S}_{12} \\ \mathcal{S}_{21} & \mathcal{S}_{22} \end{pmatrix}.$$

Using the block structure and the fact that $\mathcal{S}_{11} = 0$, we get

$$\Delta_{11} = \Delta_{12} \mathcal{S}_{22} \Delta_{21}, \quad (43)$$

$$\Delta_{12} = -\mathcal{S}_{21}^{-1}, \quad (44)$$

$$\Delta_{22} = 0. \quad (45)$$

Response function

Due to the forward-dependence of the kernels $K^{(l)}$, the off-diagonal block matrix \mathcal{S}_{21} is a lower triangular matrix and we get its inverse from forward propagation

$$\begin{aligned} \Delta_{12}^{(lm), (\alpha\beta), (\gamma\delta)} &= N^{-1} \nu_l^{-1} \delta_{lm} + 1_{l>0} \delta_{(\alpha\beta), (\gamma\delta)} \sigma_w^2 \left([\phi_\alpha^{(k-1)}]' [\phi_\beta^{(k-1)}]' + \delta_{\alpha\beta} [\phi_\alpha^{(k-1)}]'' [\phi_\beta^{(k-1)}]'' \right)_{\mathcal{N}(0, K^{(l-1)})} \\ &\quad \times \sum_{k=0}^{l-1} \Delta_{12}^{(km), (\alpha\beta), (\gamma\delta)} \times \begin{cases} \rho^2 & k \leq L \\ 1 & k = L+1 \end{cases}. \end{aligned}$$

Here, $\Delta_{12}^{lm,(\alpha\beta),(\gamma\delta)} = \text{Cov}\left(C_{(\alpha\beta)}^{(l)}, \tilde{C}_{(\gamma\delta)}^{(m)}\right)$ is the forward response function in layer l to a perturbation of the residual in layer m . Note that despite the double index $(\alpha\beta), (\gamma\delta)$, the response is always a function of covariance entries $C_{\alpha\beta}^{(l)}$ due to the appearing $\delta_{(\alpha\beta),(\gamma\delta)}$ but depends on all elements via the appearing expectation value.

We are ultimately interested in the response function with respect to the network input as a measure for network trainability. Since $\Delta_{12}^{(lm),(\alpha\beta),(\gamma\delta)}$ is with respect to the residual kernels $C^{(l)}$, we define the residual response for all intermediate network layers $1 \leq l \leq L$ as

$$\eta_{\alpha\beta}^{(l)} := \delta_{(\alpha\beta),(\gamma\delta)} \rho^2 \sigma_w^2 \langle [\phi_\alpha^{(l-1)}]' [\phi_\beta^{(l-1)}]' + \delta_{\alpha\beta} [\phi_\alpha^{(l-1)}]'' [\phi_\beta^{(l-1)}] \rangle_{\mathcal{N}(0, K^{(l-1)})} \sum_{k=0}^{l-1} \eta_{\alpha\beta}^{(k)}$$

with initial condition $\eta_{\alpha\beta}^{(0)} = d_{\text{in}}^{-1}$. Due to their additive structure the response function of the kernels $K^{(l)}$ is given by $\chi_{\alpha\beta}^{(l)} := \sum_{k=0}^l \eta_{\alpha\beta}^{(k)}$. Finally, the output response is given by

$$\chi_{\alpha\beta}^{\text{out}} = \sigma_{w, \text{out}}^2 \langle [\phi_\alpha^{(L)}]' [\phi_\beta^{(L)}]' + \delta_{\alpha\beta} [\phi_\alpha^{(L)}]'' [\phi_\beta^{(L)}] \rangle_{\mathcal{N}(0, K^{(L)})} \sum_{k=0}^L \eta_{\alpha\beta}^{(k)}.$$

Kernel fluctuations

Using Eq. (43), we get for the diagonal term

$$\Delta_{11}^{(lm)} = \sum_{k,n} \Delta_{12}^{(lk)} \mathcal{S}_{22}^{(kn)} \Delta_{21}^{(nm)}.$$

This quantity describes the Gaussian fluctuations of the residual kernels $C^{(l)}$ in networks of finite width N around the NNGP value: $C^{(l)} = C_*^{(l)} + \delta C^{(l)}$ with $\delta C^{(l)} \sim \mathcal{N}(0, \Delta_{11}^{(ll)})$. Kernel fluctuations can be used to compute finite-width corrections to quantities such as the posterior kernels, generalization error, etc. The fluctuations for the network kernels $K^{(l)}$ can be once again computed based on their additive nature as $K^{(l)} = \sum_k C^{(k)} = \sum_k C_*^{(k)} + \sum_k \delta C^{(k)}$.

Appendix C MAXIMUM ENTROPY CONDITION FOR OPTIMAL SCALING

We here derive an alternative condition for optimal signal variance, building on Bukva *et al.* [25] who proposed this method to study trainability in feed-forward networks. Their conjecture is that networks with signal distributions that are approximately uniform, or put differently maximally entropic, are more expressive.

For wide networks, the signal distribution of internal layers is approximately Gaussian

$$p(h; \sigma^2) = \frac{1}{\sqrt{2\pi\sigma^2}} \exp\left(-\frac{1}{2\sigma^2} h^2\right),$$

considering only a scalar component h here as all components h_i are independent of one another.

We here focus on the readout layer. The distribution of the post-activation $z = \phi(h)$ is then

$$p(z; \sigma^2) = \frac{1}{\sqrt{2\pi\sigma^2} \phi'(\phi^{-1}(x))} \exp\left(-\frac{1}{2\sigma^2} \phi^{-1}(z)^2\right).$$

For $\phi = \text{erf}$, the post-activation is approximately bounded by $z \in [-1, 1]$. Thus, we compute the Kullback-Leibler

divergence between the distribution of the post-activation and a uniform distribution on that interval

$$\begin{aligned}
D_{\text{KL}}(p_{\text{uni}}|p_{\phi}) &= \int_{-1}^1 dz p_{\text{uni}}(z) [\ln p_{\text{uni}}(z) - \ln p_{\phi}(z)] \\
&= \int_{-1}^1 dz \frac{1}{2} \ln\left(\frac{1}{2}\right) + \frac{1}{2} \frac{1}{2\sigma^2} \phi^{-1}(z)^2 + \frac{1}{2} \ln\left(\sqrt{2\pi}\sigma\phi'(\phi^{-1}(z))\right) \\
&= \ln\left(\frac{1}{2}\right) + \frac{1}{2} \int_{-1}^1 dz \frac{1}{2\sigma^2} \phi^{-1}(z)^2 + \ln\left(\sqrt{2\pi}\sigma\frac{2}{\sqrt{\pi}} \exp(-\phi^{-1}(z)^2)\right) \\
&= \ln\left(\frac{1}{2}\right) + \ln(\sqrt{8}\sigma) + \frac{1}{2} \int_{-1}^1 dz \left(\frac{1}{2\sigma^2} - 1\right) \phi^{-1}(z)^2 \\
&= \ln\left(\frac{\sqrt{8}}{2}\right) + \ln(\sigma) + \frac{1}{2} \left(\frac{1}{2\sigma^2} - 1\right) \int_{-\infty}^{\infty} dh \phi^{-1}(\phi(h))^2 \phi'(h) \\
&= \ln(\sqrt{2}) + \frac{1}{2} \ln(\sigma^2) + \frac{1}{2} \left(\frac{1}{2\sigma^2} - 1\right) \int_{-\infty}^{\infty} dh h^2 \frac{2}{\sqrt{\pi}} \exp(-h^2) \\
&= \ln(\sqrt{2}) + \frac{1}{2} \ln(\sigma^2) + \frac{1}{2} \left(\frac{1}{2\sigma^2} - 1\right).
\end{aligned}$$

Maximizing the Kullback-Leibler divergence amounts to

$$0 \stackrel{!}{=} \frac{\partial}{\partial \sigma^2} D_{\text{KL}}(p_{\text{uni}}|p_{\phi}) = \frac{1}{\sigma^2} - \frac{1}{4} \frac{1}{\sigma^4},$$

yielding as the condition for the signal variance before the readout layer $\sigma^2 \stackrel{!}{=} 1/4$. This condition is equivalent to the one in the Section III under the assumption that the dynamic range of the error function is given by $\mathcal{V} = 1$.

Appendix D ADDITIONAL PLOTS

A Decay of response function

Matching the observations by Yang and Schoenholz [23], the response function in ResNets decays sub-exponentially as shown in Fig. 7.

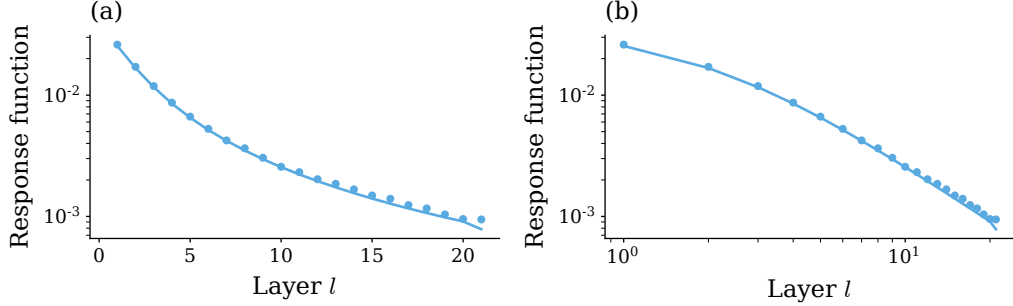


Figure 7. Log-plot (a) and log-log-plot (b) of the response function $\eta^{(l)}$ for a residual network of depth $L = 20$. Dots represent simulations over 10^2 input samples and 10^3 network initializations, solid curves show theory values. (a) The decay of the response function is sub-exponential. (b) In later layers, the decay follows a power law. Other parameters: $\sigma_{w, \text{in}}^2 = \sigma_w^2 = \sigma_{w, \text{out}}^2 = 1.2$, $\sigma_{b, \text{in}}^2 = \sigma_b^2 = \sigma_{b, \text{out}}^2 = 0.2$, $d_{\text{in}} = d_{\text{out}} = 100$, $N = 500$, $\rho = 1$.

B Input kernels for different tasks

In Section III, we study the signal propagation and scaling behavior in residual networks for different tasks. In Fig. 8, we show the normalized overlap kernels $\frac{1}{\max_{\alpha\beta} x_{\alpha} \cdot x_{\beta}} X^{\top} X$ with P data samples for the studied tasks. For MNIST, we

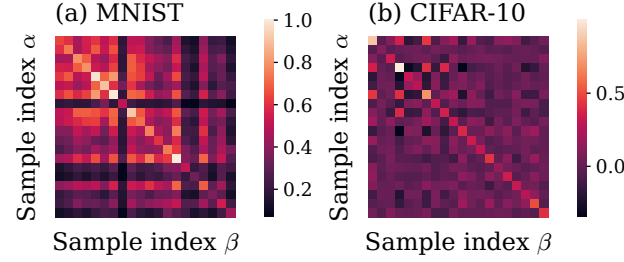


Figure 8. Normalized overlap kernels of different tasks for $P = 20$ samples. Details on the tasks can be found in the text.

consider binary classification between 0 and 3 with equal number of samples from both classes $P_0 = P_3 = \frac{1}{2}P$. For CIFAR-10, we investigate binary classification between airplanes and dogs with equal number of samples from both classes $P_{\text{airplane}} = P_{\text{dog}} = \frac{1}{2}P$.

-
- [1] A. Krizhevsky, I. Sutskever, and G. E. Hinton, Imagenet classification with deep convolutional neural networks, in *Adv. Neural Inf. Process. Syst.*, Vol. 25, edited by F. Pereira, C. J. C. Burges, L. Bottou, and K. Q. Weinberger (Curran Associates, Inc., 2012) pp. 1097–1105.
 - [2] D. Silver, A. Huang, C. J. Maddison, A. Guez, L. Sifre, G. Van Den Driessche, J. Schrittwieser, I. Antonoglou, V. Panneershelvam, M. Lanctot, *et al.*, Mastering the game of go with deep neural networks and tree search, *Nature* **529**, 484 (2016).
 - [3] K. He, X. Zhang, S. Ren, and J. Sun, Deep residual learning for image recognition, in *Proceedings of the IEEE Conference on Computer Vision and Pattern Recognition (CVPR)* (2016).
 - [4] K. He, X. Zhang, S. Ren, and J. Sun, Identity mappings in deep residual networks, in *European Conference on Computer Vision*, Vol. 9908 (2016) pp. 630–645.
 - [5] A. Krizhevsky and G. Hinton, *Learning multiple layers of features from tiny images*, Tech. Rep. (2009).
 - [6] C. Szegedy, S. Ioffe, V. Vanhoucke, and A. A. Alemi, Inception-v4, inception-resnet and the impact of residual connections on learning, in *Proceedings of the Thirty-First AAAI Conference on Artificial Intelligence*, AAAI’17 (AAAI Press, 2017) pp. 4278–4284.
 - [7] S. Ioffe and C. Szegedy, Batch normalization: Accelerating deep network training by reducing internal covariate shift, in *Proceedings of the 32nd International Conference on Machine Learning*, Proc. Mach. Learn. Res., Vol. 37, edited by F. Bach and D. Blei (PMLR, Lille, France, 2015) pp. 448–456.
 - [8] K. Huang, Y. Wang, M. Tao, and T. Zhao, Why do deep residual networks generalize better than deep feed-forward networks? — a neural tangent kernel perspective, in *Adv. Neural Inf. Process. Syst.*, Vol. 33, edited by H. Larochelle, M. Ranzato, R. Hadsell, M. Balcan, and H. Lin (Curran Associates, Inc., 2020) pp. 2698–2709.
 - [9] T. Bachlechner, B. P. Majumder, H. Mao, G. Cottrell, and J. McAuley, Rezero is all you need: fast convergence at large depth, in *Proceedings of the Thirty-Seventh Conference on Uncertainty in Artificial Intelligence*, Proceedings of Machine Learning Research, Vol. 161, edited by C. de Campos and M. H. Maathuis (PMLR, 2021) pp. 1352–1361.
 - [10] T. Tirer, J. Bruna, and R. Giryes, Kernel-based smoothness analysis of residual networks, in *Proceedings of the 2nd Mathematical and Scientific Machine Learning Conference*, Proc. Mach. Learn. Res., Vol. 145, edited by J. Bruna, J. Hesthaven, and L. Zdeborova (PMLR, 2022) pp. 921–954.
 - [11] D. Barzilai, A. Geifman, M. Galun, and R. Basri, A kernel perspective of skip connections in convolutional networks, in *The Eleventh International Conference on Learning Representations* (2023).
 - [12] J. Zhang, B. Han, L. Wynter, B. K. H. Low, and M. Kankanhalli, Towards robust resnet: A small step but a giant leap, in *Proceedings of the Twenty-Eighth International Joint Conference on Artificial Intelligence, IJCAI-19* (International Joint Conferences on Artificial Intelligence Organization, 2019) pp. 4285–4291.
 - [13] D. Arpit, V. Campos, and Y. Bengio, How to initialize your network? robust initialization for weight-norm & resnets, in *Advances in Neural Information Processing Systems*, Vol. 32, edited by H. Wallach, H. Larochelle, A. Beygelzimer, F. d’Alché-Buc, E. Fox, and R. Garnett (Curran Associates, Inc., 2019).
 - [14] S. Hayou, E. Clerico, B. He, G. Deligiannidis, A. Doucet, and J. Rousseau, Stable resnet, in *Proceedings of The 24th International Conference on Artificial Intelligence and Statistics*, Proc. Mach. Learn. Res., Vol. 130, edited by A. Banerjee and K. Fukumizu (PMLR, 2021) pp. 1324–1332.
 - [15] S. Hayou, J.-F. Ton, A. Doucet, and Y. W. Teh, Robust pruning at initialization, in *International Conference on Learning Representations* (2021).
 - [16] H. Zhang, D. Yu, M. Yi, W. Chen, and T.-Y. Liu, Stabilize deep resnet with a sharp scaling factor τ , *Mach. Learn.* **111**, 3359 (2022).
 - [17] B. Bordelon, L. Noci, M. B. Li, B. Hanin, and C. Pehlevan, Depthwise hyperparameter transfer in residual networks: Dynamics and scaling limit, in *The Twelfth Inter-*

- national Conference on Learning Representations* (2024).
- [18] G. Yang, E. J. Hu, I. Babuschkin, S. Sidor, X. Liu, D. Farhi, N. Ryder, J. Pachocki, W. Chen, and J. Gao, Tuning large neural networks via zero-shot hyperparameter transfer, in *Adv. Neural Inf. Process. Syst.*, edited by A. Beygelzimer, Y. Dauphin, P. Liang, and J. W. Vaughan (2021).
 - [19] K. Segadlo, B. Epping, A. van Meegen, D. Dahmen, M. Krämer, and M. Helias, Unified field theoretical approach to deep and recurrent neuronal networks, *J. Stat. Mech. Theory Exp.* **2022**, 103401 (2022).
 - [20] J. Zinn-Justin, *Quantum field theory and critical phenomena* (Clarendon Press, Oxford, 1996).
 - [21] J. Hertz, A. Krogh, and R. G. Palmer, *Introduction to the Theory of Neural Computation* (Perseus Books, 1991).
 - [22] A. Papoulis and S. U. Pillai, *Probability, Random Variables, and Stochastic Processes*, 4th ed. (McGraw-Hill, Boston, 2002).
 - [23] G. Yang and S. Schoenholz, Mean field residual networks: On the edge of chaos, in *Adv. Neural Inf. Process. Syst.*, Vol. 30, edited by I. Guyon, U. V. Luxburg, S. Bengio, H. Wallach, R. Fergus, S. Vishwanathan, and R. Garnett (Curran Associates, Inc., 2017).
 - [24] S. S. Schoenholz, J. Gilmer, S. Ganguli, and J. Sohl-Dickstein, Deep information propagation, 5th International Conference on Learning Representations, ICLR 2017 - Conference Track Proceedings (2017).
 - [25] A. Bukva, J. de Gier, K. T. Grosvenor, R. Jefferson, K. Schalm, and E. Schwander, Criticality versus uniformity in deep neural networks, (2023).
 - [26] S. Li, J. Jiao, Y. Han, and T. Weissman, Demystifying resnet, *CoRR* **abs/1611.01186** (2016), 1611.01186.
 - [27] Y. Furusho and K. Ikeda, Resnet and batch-normalization improve data separability, in *Proceedings of The Eleventh Asian Conference on Machine Learning*, Proc. Mach. Learn. Res., Vol. 101, edited by W. S. Lee and T. Suzuki (PMLR, 2019) pp. 94–108.
 - [28] B. Poole, S. Lahiri, M. Raghu, J. Sohl-Dickstein, and S. Ganguli, Exponential expressivity in deep neural networks through transient chaos, in *Advances in Neural Information Processing Systems 29* (2016).
 - [29] B. Hanin, Which neural net architectures give rise to exploding and vanishing gradients?, in *Advances in Neural Information Processing Systems*, Vol. 31, edited by S. Bengio, H. Wallach, H. Larochelle, K. Grauman, N. Cesa-Bianchi, and R. Garnett (Curran Associates, Inc., 2018).
 - [30] R. T. Chen, Y. Rubanova, J. Bettencourt, and D. K. Duvenaud, Neural ordinary differential equations, in *Advances in neural information processing systems* (2018) pp. 6571–6583.
 - [31] A.-S. Cohen, R. Cont, A. Rossier, and R. Xu, Scaling properties of deep residual networks, in *Proceedings of the 38th International Conference on Machine Learning*, Proceedings of Machine Learning Research, Vol. 139, edited by M. Meila and T. Zhang (PMLR, 2021) pp. 2039–2048.
 - [32] R. Barboni, G. Peyré, and F.-X. Vialard, On global convergence of resnets: From finite to infinite width using linear parameterization, in *Advances in Neural Information Processing Systems*, Vol. 35, edited by S. Koyejo, S. Mohamed, A. Agarwal, D. Belgrave, K. Cho, and A. Oh (Curran Associates, Inc., 2022) pp. 16385–16397.
 - [33] R. Barboni, G. Peyré, and F.-X. Vialard, Understanding the training of infinitely deep and wide resnets with conditional optimal transport (2024), arXiv:2403.12887 [cs.LG].
 - [34] Y. Chen, F. Liu, Y. Lu, G. Chrysos, and V. Cevher, Generalization of scaled deep resnets in the mean-field regime, in *The Twelfth International Conference on Learning Representations* (2024).
 - [35] M. B. Li and M. Nica, Differential equation scaling limits of shaped and unshaped neural networks, Transactions on Machine Learning Research (2024), expert Certification.
 - [36] P. Marion, A. Fermanian, G. Biau, and J.-P. Vert, Scaling resnets in the large-depth regime (2024), arXiv:2206.06929 [cs.LG].
 - [37] D. Balduzzi, M. Frean, L. Leary, J. P. Lewis, K. W.-D. Ma, and B. McWilliams, The shattered gradients problem: If resnets are the answer, then what is the question?, in *Proceedings of the 34th International Conference on Machine Learning*, Proc. Mach. Learn. Res., Vol. 70, edited by D. Precup and Y. W. Teh (PMLR, 2017) pp. 342–350.
 - [38] A. Zaeemzadeh, N. Rahnavard, and M. Shah, Norm-preservation: Why residual networks can become extremely deep?, *IEEE Trans. Pattern Anal. Mach. Intel.* **43**, 3980 (2021).
 - [39] Z. Ling and R. C. Qiu, Spectrum concentration in deep residual learning: A free probability approach, *IEEE Access* **7**, 105212 (2019).
 - [40] X. Zhang, R. Jiang, W. Gao, R. Willett, and M. Maire, Residual connections harm abstract feature learning in masked autoencoders (2024), arXiv:2404.10947 [cs.CV].
 - [41] D. Doshi, T. He, and A. Gromov, Critical initialization of wide and deep neural networks using partial jacobians: General theory and applications, in *Thirty-seventh Conference on Neural Information Processing Systems* (2023).
 - [42] K. Fischer, J. Lindner, D. Dahmen, Z. Ringel, M. Krämer, and M. Helias, Critical feature learning in deep neural networks, in *Proceedings of the 41st International Conference on Machine Learning*, Proceedings of Machine Learning Research, Vol. 235, edited by R. Salakhutdinov, Z. Kolter, K. Heller, A. Weller, N. Oliver, J. Scarlett, and F. Berkenkamp (PMLR, 2024) pp. 13660–13690.
 - [43] J. Lindner, D. Dahmen, M. Krämer, and M. Helias, A theory of data variability in neural network bayesian inference, (2023).
 - [44] R. Price, A useful theorem for nonlinear devices having gaussian inputs, *IRE Trans. Inf. Theory* **4**, 69 (1958).